Field patterns as game changers of the sediment connectivity

Matthieu Herpoel[a], Charles Bielders[b], Pierre Baert[a], Adrien Michez[a], Jeroen Meersmans[a], Aurore Degré[a]

[a]TERRA Teaching and Research Centre, Gembloux Agro-Bio Tech, University of Liège, Gembloux, 5030, Belgium

[b]Unité de Génie Rural, Université catholique de Louvain, Croix du Sud 2, bte2, Louvain-la-Neuve, 1348, Belgium

Keywords: Sediment connectivity; land use; parcel fragmentation; field boundaries; vegetation barriers; open agricultural landscape; soil erosion

DOI:10.1016/j.geomorph.2025.109679

1. Introduction

Soil water erosion is defined as the detachment of soil particles and their transport by water to a deposition site (sedimentation). In north-western Europe, this process primarily affects agricultural soils due to the prevalent cultivation techniques and land management practices, such as intensive soil tillage and short crop rotations, which often result in low vegetation cover (Cerdà et al., 2009; Zema et al., 2012; Panagos et al., 2015). Since the mid-20th century, the transformation of rural areas through intensification and mechanization of agriculture has led to increased hillslopes erosion, further compounded by soil compaction and land consolidation (Dotterweich, 2008). In Belgium, the change of the agricultural landscape began with the Land Consolidation Act of 1957 which aims at reorganizing fragmented land into larger, more efficient parcels to improve farming practices and potentially increased yields. This consolidation affected 600,000 ha representing one third of agricultural lands (Lambert, 1963). Today, water erosion is particularly significant in the loess belt of north-western Europe, where the silty loam soils are intensively cultivated, making them highly susceptible to erosion (Verstraeten and Poesen, 1999; Bielders et al., 2003; Evrard et al., 2007).

This process of soil erosion in fields results in negative impacts both at the field level ("on-site" or “in-field” impacts) and downstream ("off-site" impacts). On-site impacts include direct short-term damages to crops leading to reduced agricultural yields, as well as long-term degradation of soil health (Lal, 1998). Off-site impacts manifest as damages caused by mudflows to infrastructure and agricultural parcels downstream (Boardman, 1988; Bielders et al., 2003; Evrard et al., 2007), along with a deterioration in the quality of surface water bodies (Sharpley et al., 1994). In recent decades, these impacts have increased and are expected to continue growing in the future due to anthropogenic activities, such as an increase in the proportion of spring row crops, larger field sizes, intensified soil tillage, and climate change (Nearing et al., 2004; Boardman and Vandaele, 2010). Specifically, climate change leads to rising temperatures, which are expected to disrupt the hydrological cycle, resulting in more frequent high-intensity rainfall events, contributing to increased rainfall erosivity (Nearing et al., 2004; Panagos et al., 2017). Protecting soils is therefore crucial because they are a non-renewable resource on a human timescale, soil formation processes (pedogenesis) occurring on much longer timescales than soil degradation processes (Verheijen

et al., 2009). Recognizing these challenges, there is a growing movement toward sustainable agriculture (Powlson et al., 2011; Boardman and Vandaele, 2023; Strauss et al., 2023).

In north-western Europe, off-site impacts far exceed on-site impacts (Ulén et al., 2012; Boardman et al., 2019). The extent of off-site impacts is contingent upon the hydrological and sediment connectivity among various landscape elements. As suggested by Heckmann et al. (2018), in the context of soil erosion and its off-site consequences, connectivity can be defined as the degree to which a system facilitates the transfer of sediment and water in a catchment at a given moment. It highlights the role of landscape features and layout that either promote or hinder sediment detachment and transport, by connecting or disconnecting sediment transfer processes during hydrological events. Sediment connectivity refers to both the potential for sediment transfer and the mechanisms through which it occurs, encompassing all sediment sources and potential sinks within a catchment. While structural sediment connectivity focuses on physical linkages within the landscape, functional sediment connectivity refers to sediment transport processes operating across different landscape elements (Bracken et al., 2015). Over the last decades, sediment connectivity has emerged as a crucial characteristic of geomorphic systems, playing a pivotal role in advancing our understanding of hydrology and sediment dynamics (Bracken et al., 2015; Keesstra et al., 2018; Wohl et al., 2019; Najafi et al., 2021). As highlighted by Baartman et al. (2013), Mekonnen et al. (2015) and Keesstra et al. (2009, 2018), it is essential to focus on understanding sediments and flows dynamics throughout the entire catchment to decelerate and reduce sediment movements along transfer pathways. When integrated measures are strategically implemented in areas that facilitate the disconnection of landscape elements, they effectively reduce runoff velocity, runoff volume, and sediment transport, thereby efficiently addressing downstream issues related to flooding and sediment deposition (Mekonnen et al., 2015).

In agricultural landscapes, sediment connectivity is strongly influenced by the landscape layout, especially the land use configuration and fragmentation, reinforced by the presence of linear structures such as hedges, grass and wood strips, roads, and field boundaries. These features play a critical role in landscape fragmentation and in controlling sediment deposition (Van Oost et al., 2000; Evans, 2006; Follain et al., 2006; Szilassi et al., 2006; Bakker et al., 2008; Fiener et al., 2011; Chartin et al., 2013; López-Vicente et al.,

2021; Batista et al., 2022; Muñoz et al., 2024; Zhao et al., 2024). In regions fragmented by numerous small fields, delineated by linear structures, the regulation of sediment transfer is strongly influenced by the landscape fragmentation due to the inherent complexity of the resulting hydrological system. In the loess belt of north-western Europe, it has been demonstrated that field structures influence sediment loads primarily due to the effects of field boundaries, as they represent potential deposition sites (Takken et al., 1999; Beuselinck et al., 2000; van Dijk et al., 2005; Chartin et al., 2013; Boardman and Vandaele, 2016). Field boundaries, therefore, influence sediment transport, directly affecting sediment connectivity. At the catchment scale, it is furthermore essential to consider that land is not uniformly cultivated, and various crops cover the area with similar but staggered seasonal patterns (Fig. 1A). This results in a complex coexistence of surface conditions, such as soil cover or surface roughness, at any given time. When a field with low vegetative cover is located upstream of a densely vegetated field (Fig. 1B), the downstream crop can impede sediment movement due to the sudden increase in hydraulic roughness (Takken et al., 1999; Beuselinck et al., 2000; van Dijk et al., 2005). In catchments of silty loam agricultural regions, studies have reported sediment deposits at field boundaries following intense late spring storms. In these catchments, the downstream winter wheat acted as a vegetative barrier due to its more developed state compared to the upstream crop at that time (Boardman & Vandaele, 2010, 2016). As a result, upstream of a field boundary, sedimentation occurs on much steeper slopes than in the absence of a vegetative barrier at this boundary (Boardman and Vandaele, 2010). Landscape fragmentation plays a crucial role in shaping the formation and intensity of various types of water erosion, including sheet erosion, ephemeral gullies, and permanent gullies. It achieves this by shortening runoff pathways and promoting sedimentation (Boardman and Vandaele, 2010; Maugnard, 2015; Golosov et al., 2024). In Belgium, Beuselinck et al. (2000) observed that up to 28% of ephemeral gully deposits in the Belgian Loam Belt originated at field boundaries, driven by variations in vegetation roughness. It has also been shown that vegetation downstream of the boundaries can also prevent ephemeral gully formation on slopes up to 8% in loamy regions and up to 15% on the silty loam soils of the Condroz (Maugnard, 2015). Field boundaries are not always effective as sediment traps, as their performance can be compromised by their sensitivity to runoff generation and the formation of ephemeral gullies (Beuselinck et al., 2000). Additionally, the influence of field boundaries on sediment export is highly dependent on local topographic conditions.Other research has suggested that linear structures,

such as field boundaries, can also promote runoff and increase connectivity in a catchment, especially when the boundaries are (near)parallel to the flow direction (Fiener et al., 2011; Cantreul et al., 2020).

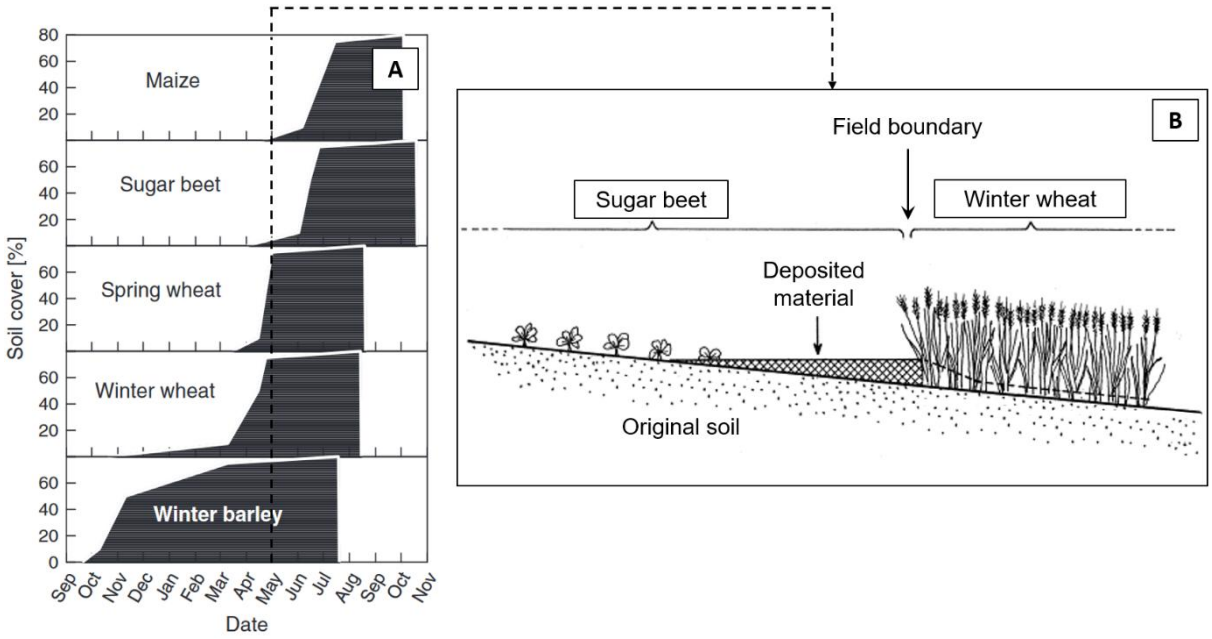

Fig. 1. (A) Typical soil cover development for different crops under Mid-European conditions (based on data from Fierner et al., 2011). (B) Sketch of the deposition pattern at the boundary between fields with a low and high vegetation cover in May (adapted from Takken et al., 1999).

The concept of patchiness remains insufficiently established and tested in the field of hydro-sedimentology. For example, studies exploring the effects of patchiness on the connectivity of agricultural landscapes are relatively scarce (*e.g.* Fiener et al., 2011; Baartman et al., 2020; Batista et al., 2022). However, evidence from some research suggests that the reduction of the field size and, consequently, the increase in patchiness have a reducing effect on surface runoff (Fohrer et al., 2005; Bormann et al., 2007; Ziegler et al., 2007). Experience from land reconsolidation projects indicates that a reduction in patchiness resulting from field enlargement increases runoff volume and peak discharge (Luft et al., 1981; Bucher and Demuth, 1985), although the diversity of changes associated with reconsolidation introduces some uncertainty regarding the specific contribution of each measure to the overall effect (Bronstert et al., 1995). In general, prevalent experimental studies on erosion, focusing either on small eroded parcels or on sediment yields

from larger catchment areas, often tend to overlook the complexity of interactions between landscape patchiness, linear structures, and sediment connectivity (Fiener et al., 2019).

Various strategies for identifying and quantifying landscape connectivity have been employed, encompassing both mapping and modelling techniques. Among these approaches, sediment connectivity indices stand out for their simplicity and ease of use, as they provide a quantitative assessment of the potential sediment transfer between different compartments within a catchment. The sediment connectivity index (IC) proposed by Borselli et al. (2008) and improved by Cavalli et al. (2013), widely used to represent structural connectivity, quantifies the potential linkage between different compartments of a catchment and indicates the probability of a particle at a certain location to reach a sink or a predefined target area. Due to its relative simplicity and ability to account for the topological sequence of landscape properties, the *IC* metric can help account for vegetation barriers on sediment trapping at the catchment scale (Cassi, 2010), filling a current gap in modelling (Gumiere et al., 2011). It is also suitable for taking into account anthropogenic structures (*e.g.* Borselli et al., 2008; Calsamiglia et al., 2017, 2018; Zhao et al., 2024). The *IC* measure incorporates the same factors as those used in travel time and sediment transport capacity calculations but takes the runoff potential of slopes and the organisation of the landscape more into account. This is particularly important when accounting for the effects of vegetation and the topological sequence of vegetation (Vigiak et al., 2012). These properties make *IC* a sensible option for studying patchiness in agricultural catchments.

The assessment of connectivity involves the concept of flow resistance, also known as impedance, which is evaluated through various methodologies incorporating land use and topographic features. The original sediment connectivity index incorporates the USLE/RUSLE C factor (Wischmeier and Smith, 1978; Renard, 1997) to derive the weighting factor (*W*), serving as an indicator of resistance to runoff and sediment transport (Borselli et al., 2008). Numerous studies have adapted this impedance factor to suit different contexts. For instance, Cavalli et al. (2013) modified this index by implementing a weighting factor based on residual topography, which is more suitable for mountainous regions. Zanandrea et al. (2020) developed a method using Manning's coefficient, which has the potential to represent impedance in forested

catchments. However, none of the existing *W* adequately account for the disconnection effects induced by landscape patchiness, particularly the orientation and position of field boundaries.

The present research investigates the impact of spatial patterns of land use and management, specifically focusing on their effects on sediment connectivity at the catchment scale, with a particular emphasis on three catchments facing soil erosion issues. The central question guiding this research is: How does the patchiness of agricultural landscapes influence sediment connectivity and, consequently, sediment transfer at the scale of small catchments? The study hypothesizes that an increased patchiness in agricultural landscapes, characterized by smaller field sizes and more diverse land use, arranged with hydrological performance in mind, reduces sediment connectivity, and thus mitigates soil erosion. Conversely, larger field sizes and homogenous land use might enhance connectivity, exacerbating erosion risks. Hence, the specific objectives of this study are as follows:

(i) Analyse at a catchment scale the impact on hydrological barriers of the current spatial distribution of crops, considering the structure of the parcel's fragmentation.

(ii) Propose an enhanced version of the Borselli et al. (2008) sediment connectivity index that integrates agricultural landscape fragmentation through parcel connectivity. This Revised index will be used to analyse how landscape patchiness, particularly fragmentation patterns and the spatial positioning of fragmenting elements, influences flow modulation across the catchment.

(iii) Promote a landscape arrangement aligned with the natural characteristics of the terrain by organising agricultural practices in harmony with the topography, thereby reducing sediment connectivity while also considering agronomic factors for optimal land management.

These investigations aim to enhance our understanding of the effects of the patchiness on connectivity and strengthen our ability to develop appropriate measures to mitigate off-site erosion impacts.

2. Study areas

The catchment has been identified as the most suitable spatial scale for studying hydrological processes (Brocca et al., 2012). Land management strategies are often designed at the field scale (*e.g.* Maugnard et al., 2013; Prasuhn et al., 2013) or at the scale of large catchments (*e.g.* Borrelli et al., 2021), while the intermediate scale of the small catchment is sometimes overlooked. Hence, an examination of landscape patchiness will be undertaken across multiple small catchments, each featuring distinct agricultural contexts to explore the regional variations in land use, agricultural practices, and the configuration of agricultural parcels.

The three study catchments (Fig. 2) are sub-catchments of the Scheldt (50°41'43.66" N, 3°26'7.67" E), the Dyle (50°37'47.56" N, 4°36'59.37" E) and the Houyou (50°26'28.88" N, 5°12'51.93" E) located in Wallonia (Belgium) in different land use contexts (Table 1). The study sites are located on the silt loam (Scheldt and Dyle) and Condroz (Houyou) agro-pedological regions, which are highly vulnerable to surface sealing and water erosion (Verstraeten and Poesen, 1999; Verstraeten et al., 2006; Maugnard et al., 2013, 2014) as well as to muddy floods (Bielders et al., 2003; Evrard et al., 2007). The three sub-watersheds lack permanent watercourses. The mean annual temperature across the three watersheds ranges from 9 to 10°C, while mean annual precipitation ranges from 700 to 900 mm (Evrard et al., 2008). In the Belgian loess belt, the rate of erosion can vary from a few tons ha-1 yr-1 to more than 100 t ha-1 yr-1 (Ryken et al., 2018).

The Scheldt sub-catchment covers 1,645 ha within the Belgian loess belt and is predominantly situated in Celles, Hainaut province. The dominant soil types are Luvisols, featuring a sandy loam and silt loam texture with good natural drainage. This catchment is primarily used for agriculture, comprising 89% of the land, including 19% for grassland and forage. It also encompasses small areas designated for built-up (5%) and forested regions (6%). Winter wheat (*Triticum aestivum*; 24%), sugar beet (*Beta vulgaris*; 11%), and potatoes (*Solanum tuberosum*; 10%) are the most cultivated crops. Altitude varies from 21 to 147 meters, with the terrain displaying flatter characteristics in the north and becoming more undulating in the south, and the average slope gradient across the area is 4.5%.

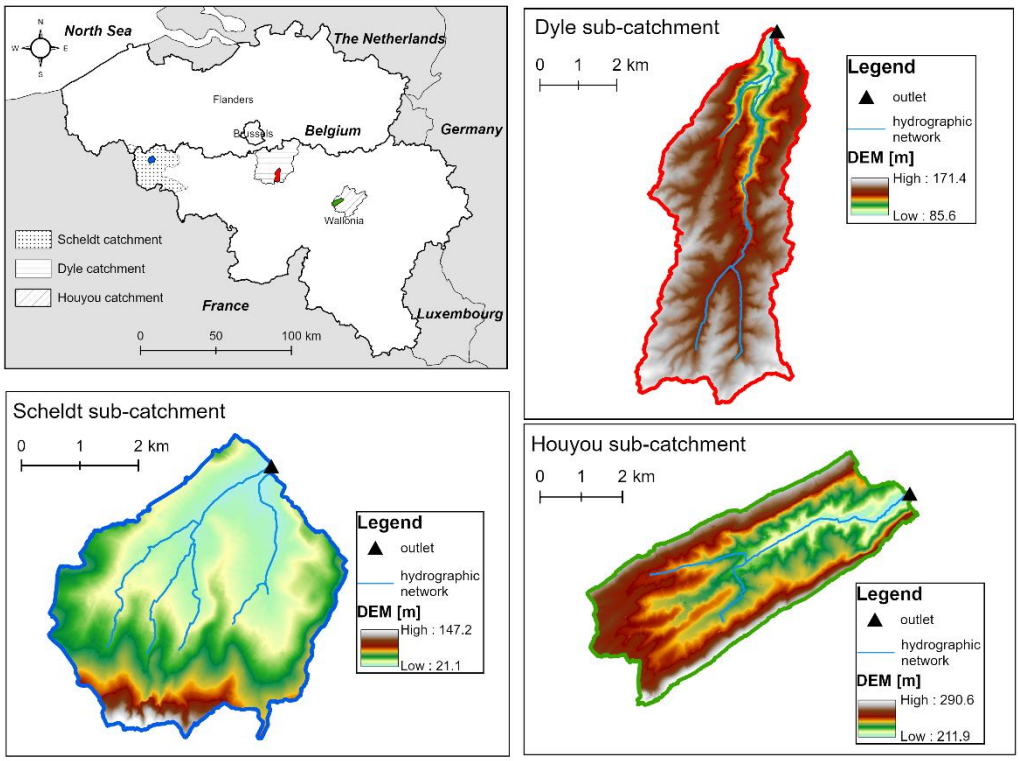

Fig. 2. Presentation of the study areas [location, digital elevation model (DEM), hydrographic network and outlet].

The Dyle sub-catchment encompasses 2,614 ha within the Belgian loess belt, primarily located in Chastre in the Walloon Brabant province. The prevalent soils in this area are Cambisols and Luvisols, both derived from Quaternary loess. Approximately 85% of the land is dedicated to arable farming, including 11% for grassland and forage, with smaller portions allocated to built-up areas (4%) and forests (9%). The principal crops grown here consist of winter wheat (30%), sugar beet (13%), and potatoes (10%). The altitude ranges from 86 to 172 meters, and the terrain is characterized by gentle slopes, with an average slope gradient of 5%.

The Houyou sub-catchment spans 2,093 ha and covers the town of Ohey in the Namur province. The challenges of erosion in this mid-plateau area are greater due to shallower soils. The dominant soil types are "Luvisols" characterized by silt loam and stony silt loam textures. Most of this catchment, approximately 85%, is dedicated to arable farming, with 29% allocated for grassland and forage. Additionally, there are minor areas occupied by forest (10%) and built-up regions (4%). The primary crops cultivated here include

winter wheat (24%), maize (*Zea mays*; 12%), and sugar beet (7%). Altitude varies from 212 to 291 meters, and the topography exhibits a marked NE-SW orientation. In this undulating landscape, the average slope gradient is 6%.

Table 1. Characteristics (mean and standard deviation, stdev) of land use over the period 2018 and 2022 in the three sub-catchments. The data are averages over the five-year period. Q50 and Q95 correspond to the 50th (=median) and 95th percentile, respectively.

Landscape characteristics	**Units**	**Scheldt**		**Dyle**		**Houyou**	
		Mean	Stdev	Mean	Stdev	Mean	Stdev
Land use							
Catchment area	ha	1,645	-	2,614	-	2,093	-
Wooded area	%	6	0.08	9	0.17	10	0.13
Built surface	%	5	0.15	4	0.11	4	0.15
Agricultural area	%	89	0.15	85	0.16	85	0.15
Spring row crops	%	37	2.3	35	2.1	26	0.6
Winter crops	%	33	2.3	39	2.1	30	0.8
Grasslands	%	19	0.6	11	0.5	29	1.1

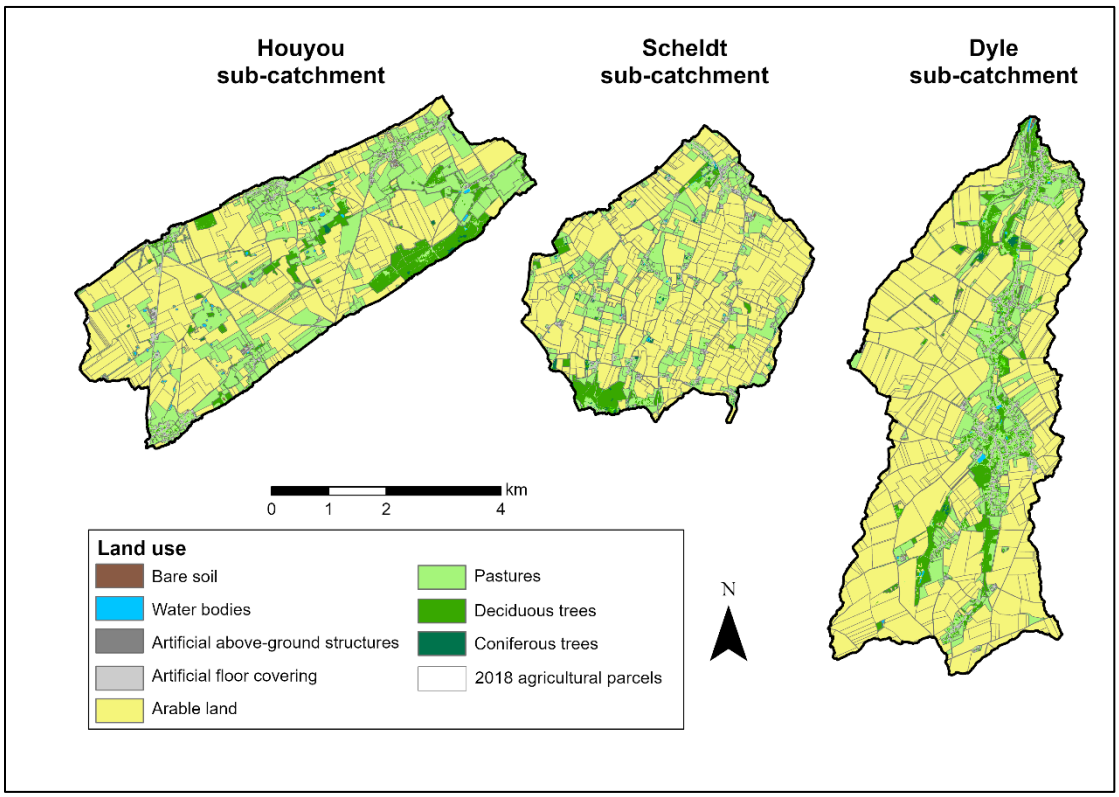

214 **Fig. 3.** Maps of land use and agricultural parcels in the three sub-catchments for the year 2018 at a scale
215 of 1:60,000.

216

217 # 3. Methodology

218 ## 3.1. Data sources

219 The dataset used for this study comprises a 2013-2014 Digital Terrain Model (DTM) with a 1 m resolution
220 and an altimetric accuracy of around 0.12 m in absolute terms, covering the entire region of Wallonia. It
221 also comprises a map of the hydrographic network and the 2018-2022 Land Parcel Identification System
222 (LPIS), which catalogues annually declared agricultural parcels. These parcels encompass both arable
223 lands used for crops and non-productive areas such as grasslands, fallow land and vegetated strips. All
224 data were sourced from the Walloon geoportal WalOnMap (available at https://geoportail.wallonie.be).
225 Additionally, land use maps at 2 m spatial resolution from the 2018-2022 LifeWatch dataset for Wallonia are
226 utilised (Radoux et al., 2022).

227

3.2. Current state of the patchiness effect in the Walloon agricultural landscape

To analyse the influence of landscape patchiness in the three sub-catchments, we compiled a dataset covering potential vegetation barriers for the years 2018 and 2021. These years were selected as they offer a representative snapshot of the typical land use patterns across the parcels during the five-year study period (2018-2022). A potential vegetation barrier is defined as the intersection between a concentrated flow path and the boundary between two fields (Fig. 4). The term "potential" is used because the barrier effect is time dependent. These vegetation barriers are further characterized by the crop type upstream of the potential barrier, that may be underdeveloped and prone to runoff, and crop type downstream of the potential barrier that may act as a hydraulic brake depending on the cropping season. For each potential vegetation barrier, a reclassification is conducted based on crop category groups: winter crops, spring row crops, and grassland. Each potential vegetation barrier is associated with an upstream contributing area. Three categories of contributing areas are used, classified in ascending order of surface area: small (≥0.1 ha), medium (≥1 ha), and large (≥10 ha). Concentrated runoff is considered downstream of a contributing surface area of 1 ha.

The potential vegetation barriers dataset has also been categorized based on the angle formed between the field boundary and the upstream flow path (Fig. 4). Three distinct classes were derived based on observations across the three catchment areas, though their applicability has not been tested in other catchments. The data reveal that in over 90% of cases, when the angle is 45° or greater, the flow path crosses the field boundary. Conversely, when the angle is below 30°, the flow path runs parallel to the boundary, also observed in over 90% of cases. Any anomalies or exceptions are addressed through manual reclassification. The final classification consists of the following three categories:

- ≥45°: it is considered that in this case the stream crosses the potential vegetation barriers.
- ≤30°: it is considered that in this case the stream flows along the field boundary

- 30°< & <45°: the flow may or may not cross the boundary. These uncertain potential vegetation barriers, in the minority (≤11%), were not considered in this study.

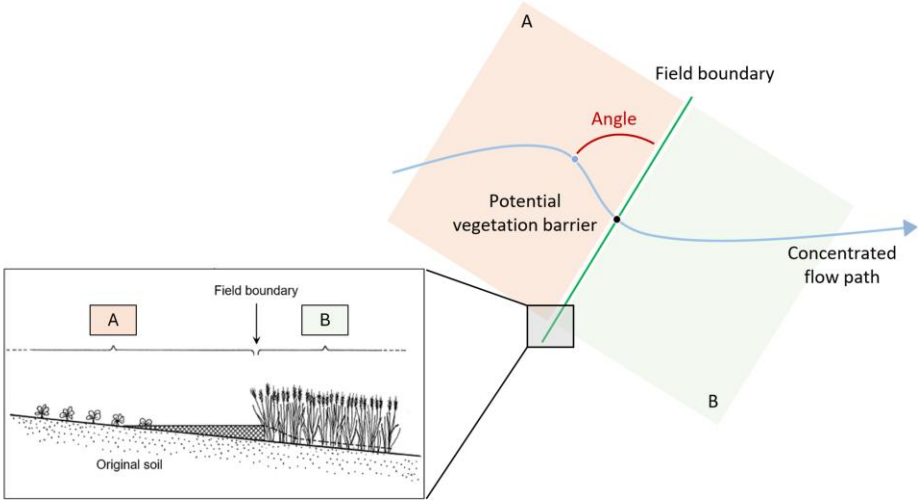

Fig. 4. Diagram illustrating the potential vegetation barrier from an upstream field (A) to a downstream field (B). The angle is measured between the concentrated flow path and the boundary between the adjacent parcels, with the intersection point, defined as the potential vegetation barrier, serving as the vertex. The angle ranges from 0 to 90 degrees.

In our examination of the flow disconnection effects induced by the agricultural landscape patchiness, our focus is on potential vegetation barriers that counter the runoff flow (≥45°). When the angles are less than or equal to 30°, no potential vegetation barrier is present. As specified by Fiener et al. (2011) and Cantreul et al. (2020), field boundaries that run parallel to flow paths do not reduce runoff within the landscape. The density (number per unit area) of these potential vegetation barriers within a catchment serves as an indicator of the arrangement and dimensions of land parcels.

The data will be standardised according to the agricultural area of the different catchment areas to ensure a fair and relevant comparison between the catchments studied.

3.3. Sediment connectivity index

3.3.1. Computation of the index of connectivity

The sediment connectivity index (IC), defined by Borselli et al. (2008), is a pixel based dimensionless indicator that assesses the potential for sediment delivery from production areas (e.g. agricultural slopes) to sinks (e.g. river network) (Eq. 1). This index is mainly derived from a DEM and the surface runoff impedance associated with different land uses and, therefore, aims to assess the topographical and land cover control on sediment transfer processes:

$$IC = log_{10}\left(\frac{D_{up}}{D_{dn}}\right) \quad \textit{(Eq. 1)}$$

Where D_{up} and D_{dn} represent the upslope and downslope components of connectivity (Fig. 5), respectively. *IC* is defined within the interval [-∞, +∞], with higher *IC* values indicating increased connectivity. The upslope component, D_{up}, signifies the potential sediment transport downstream from the upstream area and is estimated as follows (Eq. 2):

$$D_{up} = \overline{WS}\sqrt{A} \quad \textit{(Eq. 2)}$$

Where $\overline{W}$ is the average upstream area weighting factor (dimensionless), $\overline{S}$ is the average slope of the upstream area (m/m), and A is the upstream surface area (m²). The downslope component, D_{dn}, considers the slope-weighted distance and the weighting factor of each pixel that the particle must travel to reach the nearest target or sink. Therefore, D_{dn} can be expressed as follows (Eq. 3):

$$D_{dn} = \sum_i \frac{d_i}{W_i S_i} \quad \textit{(Eq. 3)}$$

Where d_i is the length of the flow path along the i-th cell in the steepest downhill direction (m), and W_i and S_i are the weighting factor and slope gradient of the i-th cell, respectively.

The calculation of *IC* was carried out with the 'Connectivity-Index-ArcGIS-toolbox' (Cavalli et al., 2014). *IC* was computed in reference to the catchment's hydrographic network, using a DTM from 2013-2014 with a resolution of 1 m as suggested by Cantreul et al. (2018). This pixel size enabled these authors to locate all

291 “key areas” in terms of erosion as well as to better account for the impact of linear features in the catchment
292 (*e.g.* grass strips and roads). To enhance the hydrological analysis of water flow pathways, the DTM must
293 undergo a pre-processing stage in order to be hydrologically correct (O’Callaghan and Mark, 1984; Jenson
294 and Domingue, 1988). Lidberg et al. (2017) caution that the fill method, suggested by Cavalli et al. (2014),
295 may falter with DTMs of higher resolution. The fill process can inadvertently generate linear, artificial
296 streams, diverging from the natural watercourse patterns. To counteract this, the optimized pit removal
297 (OPR) technique is employed, which combines breaching and filling approaches to preserve the intricate
298 topographical nuances of the landscape (Soille, 2004). This advanced method was employed in the pre-
299 processing phase for DTMs, ensuring a more accurate representation of the water flow pathways. *IC* and
300 OPR were both computed in *ArcGIS 10.8.1*.

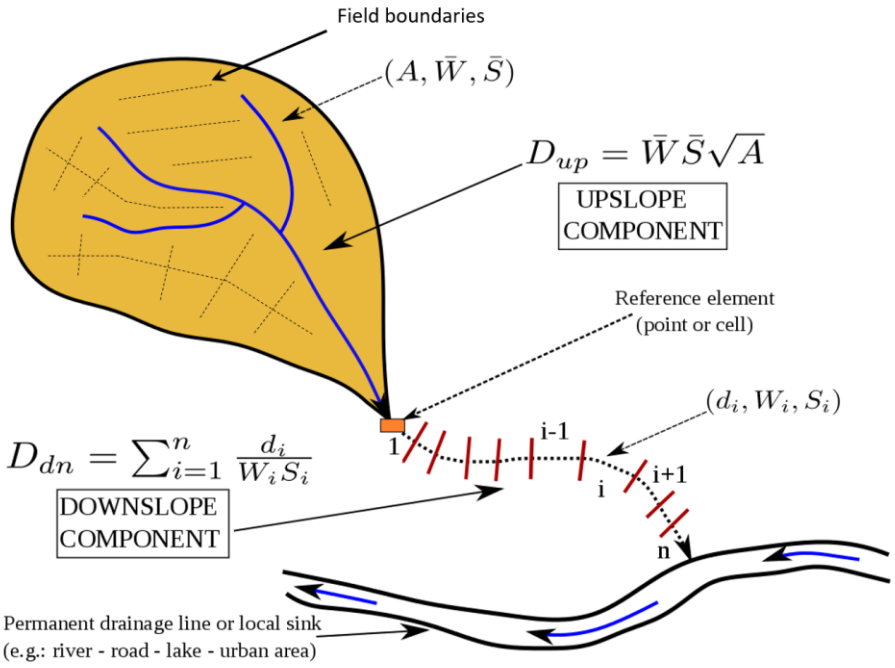

301 **Fig. 5.** Definition of the upslope and downslope components in the landscape for index of connectivity, and
302 adjustment of the weighting factor to account for agricultural fragmentation (adapted from Borselli et al.,
303 2008).

304

305 *3.3.2. Adjusting the weighting factor*

306 Modifications to the original Borselli et al. (2008) model, revised by Cavalli et al. (2013), were designed to
307 incorporate the effect of landscape patchiness, and specifically connectivity between parcels, into the model

(Fig. 5). To account for sediment retention effects at the boundaries between two fields, the weighting factor (*W)* has been enhanced. *W*, featured in both the upslope and downslope components of *IC* within equations (2) and (3), was initially proposed by Borselli et al. (2008) to simulate the impedance to runoff and sediment flows attributed to the characteristics of local land use and the physical properties of the land surface. Borselli et al. (2008) recommend using the C factor from the USLE-RUSLE models (Wischmeier and Smith, 1978; Renard, 1997) as a weighting factor (Table 2) for regions where vegetation cover and land use management significantly influence sediment fluxes, such as in our study area. The C factor represents the effect of surface cover and roughness on soil loss. However, this weighting factor only considers the effect of land cover and not the effect of linear features associated to parcel configuration on soil loss.

Table 2. C factor (0: no erosion possible and 1: maximum erosion with bared soil).

Agricultural land uses	**C factor**	**Land uses**	**C factor**
Crop groups*		***Artificial surfaces****	
Perennial grassland	0.01	Artificial covering (on the ground)	0.001[a]
Perennial fruit crops (apples, pears, ...)	0.05	Artificial covering (above-ground)	0
Temporary grassland	0.10		
Winter cereals	0.25	***Others****	
Winter rape, summer cereals, flax, peas	0.30	Forest area	0.001
Potatoes (early), beetroot, turnips, spinach, ...	0.35	Water bodies	0
Potatoes (late), chicory, celeriac, leeks, beans, ...	0.40	Bare ground	1
Maize, cabbage, ...	0.45		
Asparagus, strawberries, carrots, ...	0.50		
Ornamental plants, courgettes, pumpkins, ...	0.60		
Arboriculture	0.70		
Onions, chives	0.80		

* Swerts et al. (2020) ** Wischmeier & Smith (1978) [a] A non-zero value is assigned to this category to ensure continuity on both sides of the road network.

A new parameter, the parcel connectivity (*P*), is introduced to account for the sediment connectivity between parcels. *P* is a dimensionless parameter ranging from 0 to 1. This enhanced approach better captures the hydrological nuances specific to field boundaries, thereby contributing to a more accurate assessment of the impact of landscape patchiness on sediment retention. It is integrated into the $\overline{W}$ parameter of the upslope component, where the calculation of the upstream area for the i-th cell, always weighted by the C factor, will now also consider this connectivity factor. The connectivity factor is applied to boundary pixels only when the flow crosses the boundary and is omitted when the flow runs parallel to it. Specifically, a connectivity of 30% ($P = 0.3$) is applied at these boundaries to capture the hydraulic braking effect induced by the vegetation barriers (Gumiere et al., 2011; Muñoz et al., 2024). That means, a flow crossing a field boundary will be reduced by 70%, allowing 30% of the flow to pass through. This parcel connectivity of 30% is the value used in Belgium following numerous field observations (Oorts et al., 2020; Swerts et al., 2020). In this study, *P* is applied independently of the land cover on either side of the field boundary. Thus, the presence of a boundary will be reflected in the *IC* through the new weighting of the upstream area in the upslope component. In comparison, the Borselli index represents connectivity in the absence of landscape fragmentation.

3.4. Scenarios testing various land use configurations and parcel layouts

The connectivity index of Borselli et al. (2008) will be used to compare various scenarios of land use and parcel configuration (Fig. 6). For the scenarios tested, only the agricultural areas, including grassland and cropland, will be reorganised to assess the impact of the agricultural parcel patchiness on sediment connectivity.

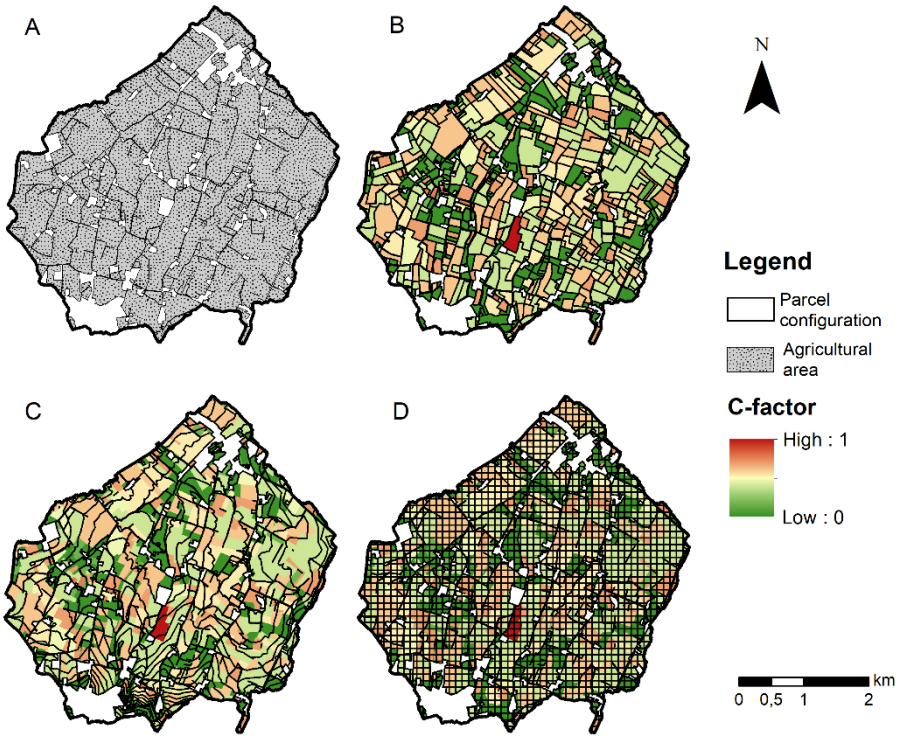

Fig. 6. Parcel configuration and crop rotation scenarios studied in the Scheldt sub-catchment: A) a unified structure for land use analysis, B) the 2018 parcel setup, C) fragmentation along 5 m isolines, and D) 1 ha grid divisions.

This study focuses on two key factors: land use and the spatial configuration of agricultural parcels, including both their size and geometry, within the catchment areas. A differentiation is established between existing parcel configurations and theoretical scenarios (Table 3). In the case of existing configurations, *IC* will be calculated for the year 2018, which will serve as a reference for existing scenarios (Fig. 6b). First, land use will be evaluated without considering crop patchiness by aggregating the entire agricultural area and designating a single land use type (Fig. 6a). Five land-use types will be analysed, ranked in ascending order of soil protection by plant cover with their respective C factor of crops in Wallonia (Table 2; Swerts et al., 2020): bare soil (C factor = 1), spring crops (C factor = 0.4), winter cereals (C factor = 0.25), temporary grassland (C factor = 0.1), and permanent grassland (C factor = 0.01). Second, the structural characteristics of the agricultural landscape will be assessed through various scenarios that modify the fragmentation of the agricultural area (Table 3). Three configurations will be examined: the 2018 parcel configuration (Fig. 6b), a 1-hectare square grid to assess the impact of small parcel size on connectivity (Fig. 6d), and a

configuration designed to cultivate across slopes following isolines, akin to contour farming practices (e.g. Farahani et al., 2016), with a subdivision of parcels based on 5 m isolines (Fig. 6c). To assess the effect of spatial pattern on connectivity, we will maintain the same land use as in 2018 for the parcel configuration scenarios, ensuring that only the structure varies. Additionally, for each configuration, parcels smaller than 100 m² were aggregated, as they are considered artifacts of the redrawing process and not representative of agricultural parcels.

Table 3. Summary of land use and parcel arrangement scenarios in the three sub-catchments for which connectivity will be assessed. $\bar{A}$ (ha) represents the average parcel area, $\bar{C}$ (-) is the average C factor in the catchment, and *Crops* (-) is the number of different crop groups characterised by an identical C factor value (Table 2). Standard deviation values are shown in brackets. The parcel configuration scenarios utilize the same land use patterns as those observed in 2018.

Scenarios	**Scheldt**			**Dyle**			**Houyou**		
	$\bar{A}$	$\bar{C}$	*Crops*	$\bar{A}$	$\bar{C}$	*Crops*	$\bar{A}$	$\bar{C}$	*Crops*
Land use									
Bare soil	14.6 (26)	0.861 (0.346)	0	16.9 (29.8)	0.822 (0.381)	0	20.7 (46.9)	0.872 (0.335)	0
Spring crops	14.6 (26)	0.345 (0.138)	1	16.9 (29.8)	0.330 (0.154)	1	20.7 (46.9)	0.349 (0.136)	1
Winter cereals	14.6 (26)	0.217 (0.088)	1	16.9 (29.8)	0.208 (0.099)	1	20.7 (46.9)	0.220 (0.089)	1
Temporary grassland	14.6 (26)	0.085 (0.039)	1	16.9 (29.8)	0.082 (0.048)	1	20.7 (46.9)	0.087 (0.047)	1
Permanent grassland	14.6 (26)	0.008 (0.022)	1	16.9 (29.8)	0.010 (0.034)	1	20.7 (46.9)	0.008 (0.037)	1
Parcel layout									
2018 land use	2.0 (2.3)	0.230 (0.169)	8	3.2 (4.1)	0.234 (0.157)	7	2.8 (3.6)	0.176 (0.162)	7
1 ha grid	0.8 (0.3)	0.230 (0.169)	8	0.8 (0.3)	0.234 (0.157)	7	0.8 (0.3)	0.176 (0.162)	7
Isoline 5m	3.4 (7.1)	0.230 (0.169)	8	3.1 (6.1)	0.234 (0.157)	7	3.6 (5.9)	0.176 (0.162)	7

3.5. Validation of connectivity

The validation of sediment connectivity indices is widely acknowledged as a critical yet complex aspect of sediment dynamics research, as emphasized by Hooke and Souza (2021). Although direct field measurements remain the most reliable approach, they require extensive data and controlled conditions, which are not always feasible. As an alternative, numerous studies (e.g., Borselli et al., 2008; Cavalli et al., 2013; Cantreul et al., 2018) have successfully employed remote sensing data and aerial photographs, particularly following significant rainfall events, to validate IC outputs.

Cantreul et al. (2018) investigated sediment connectivity within a gauged experimental catchment located in the Dyle sub-catchment. Using an orthophotoplan dated March 13, 2017, following a rainfall event of 31.7 mm, and supplemented by field observations, they demonstrated that IC predicted most areas of high, medium, and low connectivity. In addition, we leveraged an aerial image from July 21, 2021, captured after multiple extreme rainfall events, which cumulatively amounted to 241.4 mm over the preceding month and 58.9 mm in the prior week. This provided an ideal opportunity to assess the functional connectivity under extreme hydrological conditions. The aerial image and field observations (e.g. photographs of deposits) are used as ground true information in order to validate and assess the quality of the index outputs.

4. Results and discussion

In this section, we start by analysing the current state of the patchiness effect in the Walloon agricultural landscape by assessing how parcel organization, particularly the role of natural vegetative barriers created by field boundaries, affects sediment dynamics. Subsequently, we evaluate the effectiveness of both the Borselli and Revised sediment connectivity indices, comparing their capacity to capture the impacts of varying parcel configurations. Next, we validated the connectivity patterns by analysing functional connectivity, focusing on how well the indices reflect sediment flow dynamics under real-world conditions. Finally, we discuss strategic approaches to align agricultural land use with natural topography, aimed at optimizing landscape connectivity and mitigating erosion.

4.1. Current state of the patchiness effect in the Walloon agricultural landscape

In terms of land use, the allocation of land to spring crops, winter crops, and grassland remained relatively stable (Table 1). Grassland, which provides continuous year-round soil cover, accounted for an intermediate proportion in the Scheldt sub-catchment (19%), a lower proportion in the Dyle (11%), and a higher proportion in the Houyou (29%). In contrast, spring row crops, which offer less soil cover, were more prevalent in the Scheldt (37%) and Dyle (35%) sub-catchments and less so in the Houyou (26%).

Among the three sub-catchments, the Scheldt stood out as the most fragmented, with an average parcel size of 1.9 ha and a parcel density of 0.51 ha-1 (Table 4; Fig. 3). This contrasts with the Dyle and Houyou sub-catchments, which were less fragmented and characterized by larger but fewer parcels, with average cropland parcel sizes of 3.8 ha and parcel densities of 0.31 and 0.36 ha-1, respectively. The largest parcels (Q95) in the Scheldt were smaller, averaging 6 ha, compared to 10.4 ha and 11.1 ha in the Dyle and Houyou sub-catchments, respectively. The number of parcels has increased in all three catchments. Between 2018 and 2022, the Scheldt sub-catchment had a growth rate of 8.6%, while the Dyle and Houyou sub-catchments showed a smaller rise of 4% and 2.3%, respectively. This results mainly from the introduction of new vegetative strips. These characteristics highlight that the Dyle sub-catchment is the least fragmented, with relatively poorer ground cover. This results in reduced landscape heterogeneity, which in turn diminishes the effectiveness of the landscape in disconnecting surface flows.

Table 4. Characteristics (mean and standard deviation, stdev) of parcel layout over the period 2018 and 2022 in the three sub-catchments. The data are averages over the five-year period. Q50 and Q95 correspond to the 50th (=median) and 95th percentile, respectively.

Parcel layout	Units	Scheldt		Dyle		Houyou	
		Mean	Stdev	Mean	Stdev	Mean	Stdev
Average parcel size	ha	1.9	0.07	3.1	0.05	2.8	0.04
Average parcel size (excluding grassland)	ha	2.4	0.06	3.8	0.08	3.8	0.10
Q50 parcel size	ha	1.21	0.10	1.65	0.06	1.38	0.06
Q95 parcel size	ha	6.0	0.09	11.1	0.43	10.4	0.51
Number of parcels	-	738	27.1	691	10.8	650	9.6
Parcel density	ha-1	0.51	0.012	0.31	0.005	0.36	0.005

The density of potential vegetation barriers is influenced by catchment morphology and agricultural parcel fragmentation (Table 5). Across the three catchments studied, the number of potential runoff barriers remains relatively low (<0.3 ha-1). The Scheldt sub-catchment shows an intermediate barrier density of 0.24 ha-1, compared to 0.16 ha-1 in the Dyle (the lowest), and 0.27 ha-1 in the Houyou (the highest). These figures align with the densities of field boundaries and concentrated flow paths, with values of 71.7 and 74.8 m ha-1 for the Scheldt, 69.8 and 62.9 m ha-1 for the Dyle, and 86.6 and 81.4 m ha-1 for the Houyou, respectively. Despite these differences, no statistically significant correlation ($p > 0.05$) was found between vegetation barrier density and parcel or catchment characteristics. The Dyle and Houyou sub-catchments, though more elongated than the compact Scheldt, show no strong spatial resemblance. These variations in morphology, particularly in shape and size, influence the average contributing area of the vegetation barriers.

Table 5. Comparison of the dataset on potential vegetation barriers in the sub-catchments [agricultural area (A), number of potential barriers with a contributing area of ≥1 ha (n_b), and the density of potential vegetation barriers (n_b/A)] with the morphological characteristics of the catchment [Gravelius compactness index (KG) and density of concentrated flow paths with a contributing area of ≥1 ha (L_c/A)] and the agricultural parcel

patchiness [density of field boundaries which form obstacles to the flow paths (L_b/A), number of parcels (n_p), and parcels density (n_p/A)]. The data are the average of values from 2018 and 2021.

Sub-catchment	Vegetation barriers		Catchment characteristics		Parcel characteristics	
	n_b/A (ha-1)	Average contributing area (ha)	*KG*	L_c/A (m ha-1)	L_b/A (m ha-1)	n_p/A (ha-1)
Scheldt	0.24	8.6	1.23	74.8	71.7	0.51
Dyle	0.16	10.8	1.37	62.9	69.8	0.29
Houyou	0.27	13.1	1.54	81.4	86.6	0.36

The orientation of field boundaries relative to concentrated flow paths is also a key factor in assessing the disconnection potential of an agricultural landscape. For example, the 2018 parcel configurations (Fig. 6b) had a considerable proportion in terms of length of field boundaries (16.5% of the length for the Scheldt sub-catchment and 5% for the Dyle and Houyou sub-catchments) which were located along the flow concentration pathways and were therefore not considered to be obstacles. This high proportion of field boundaries in the Scheldt sub-catchment explains why the Houyou sub-catchment has the highest field boundary density at 86.6 m ha-1, despite not being the most fragmented landscape.

The Scheldt sub-catchment, characterized by the most fragmented agricultural landscape, with smaller average parcel sizes (1.9 ha) and a higher parcel density (0.51 ha-1), shows an intermediate density of potential vegetation barriers. As expected, the Dyle sub-catchment, which has the least fragmented landscape, exhibits the lowest density of potential vegetation barriers. This can partly be attributed to its larger average parcel size (3.1 ha), resulting in a lower parcel density (0.29 ha-1), combined with the least dense network of concentrated flow paths, at 62.9 m ha-1. In contrast, the Houyou sub-catchment has the highest density of vegetation barriers, despite not having the most fragmented landscape. With an average parcel size of 2.8 ha and an intermediate parcel density of 0.36 ha-1, the higher vegetation barrier density is largely influenced by the high density of concentrated flow paths (81.4 m ha-1), its linear hydrological network, and its elongated shape. The dominant surface water flow direction runs from southwest to northeast, and the concentrated flow paths, which run perpendicular to the main direction, interact with the

orientation of agricultural parcels. Many parcels are aligned across the slope gradient, which increases the density of potential vegetation barriers, enhancing their presence in the landscape. Therefore, the difference between the Scheldt and Houyou sub-catchments can be attributed to the orientation of field boundaries within the landscape, which directly affects the potential vegetation barrier density. This density thus serves as an indicator of landscape patchiness, accounting for both parcel fragmentation and the position of field boundaries.

The analysis reveals that, on average, more than 40% of potential vegetation barriers in each catchment consist of adjacent fields with the same crop category (Fig. 7). This finding suggests potential for optimizing land use within the parcels to enhance flow disconnection. In 2018 and 2021, the percentage of potential vegetative barriers with a contributing area between 0.1 and 10 ha, located between two spring crops — which are more vulnerable to erosion during heavy rainfall events— was 16.9 ± 1.25% in the Scheldt sub-catchment, 18.8 ± 1.37% in the Dyle sub-catchment, and 7.5 ± 0.72% in the Houyou sub-catchment. Regarding potential vegetation barriers situated along the most concentrated flow paths (>10 ha), a reduction to 9.6% is observed for the Scheldt sub-catchment, while an increase is seen for the Dyle and Houyou sub-catchments, reaching 21.6% and 8.8%, respectively. This percentage shows significant variation between the catchments, primarily due to differences in crop rotation practices. For instance, the Houyou catchment has a 10% lower proportion of land dedicated to spring crops compared to the other catchments, resulting in a lower frequency of potential vegetation barriers between two spring crops. Evans (2006) and Maugnard (2015) have highlighted that boundaries between fields of the same crop type minimally impact flow disconnection and sedimentation. Additionally, research by Van Oost et al. (2000) and Maugnard (2015) demonstrated that deposits are more likely to occur along boundaries between fields with different crops. These findings highlight the need for coordinated crop rotation plans, particularly on critical sections of the flow paths.

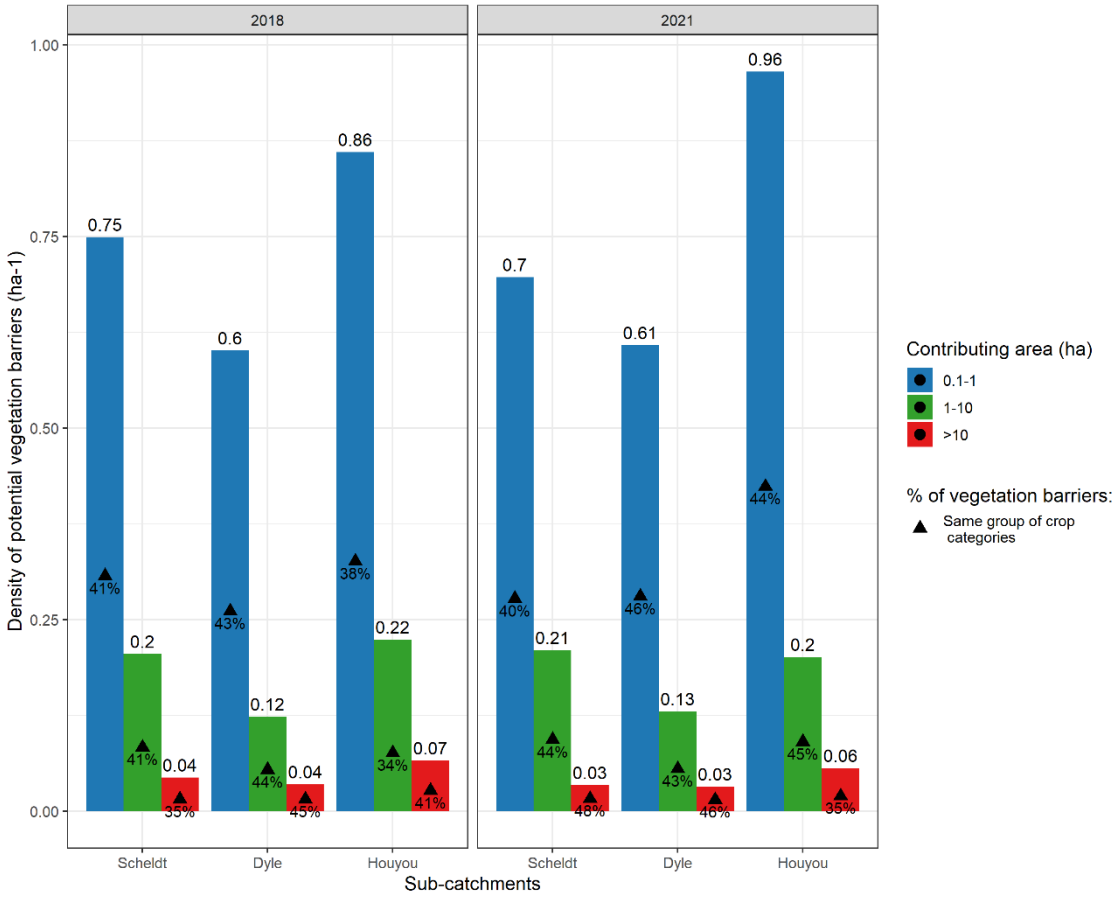

481 **Fig. 7.** Density of potential vegetation barriers (classified by contributing area) in the three sub-catchments
482 for 2018 and 2021. Triangles correspond to the percentage of potential vegetation barriers with the same
483 group of crop categories.

484

485 Despite changes in parcel structures, such as splitting, merging, or the disappearance of certain agricultural
486 parcels, and variations in crop distribution due to rotations, the density of potential vegetation barriers
487 remained relatively stable between 2018 and 2021 (Fig. 7). The parcel configurations for 2018 and 2021
488 reflect the influence of political and economic decision-making processes, which aim to balance agricultural
489 practices with land management policies (Devátý et al., 2019). This stability highlights persistent landscape
490 patterns that could benefit from targeted interventions designed to reduce connectivity and mitigate
491 sediment transport.

492

4.2. Connectivity from the Revised index and comparison with Borselli connectivity index

In the standard *IC* calculation method, sediment flow resistance is incorporated into the weighting factor (W) by adjusting the contributing area. Figure 8 compares the effects of different weighting methods for the contributing area in the Dyle sub-catchment.

Without any weighting (Fig. 8A), the contributing area at the outlet is 36.4 ha. By comparison, the Borselli Index (Fig. 8B) weights the contributing area according to the C factor, where a pixel with a C value of 1 transmits the full flow downstream. Conversely, if a pixel is covered by vegetation, flow passing through it is weighted by its C value. This weighting method results in a contributing area of 10.3 ha at the outlet. Weighting for 30% connectivity at field boundaries (Fig. 8C), for a hypothetical configuration fragmented into 1 ha parcels (Fig. 8D), reduces the outlet's contributing area to 0.61 ha. The Revised Index calculation (Fig. 8D), combining weightings from methods B and C, reduces the outlet's contributing area to 0.18 ha. In this example, the weighting method based on landscape fragmentation (Fig. 8C) has a much greater impact on the outlet's drained area than the land-use-based weighting method (Fig. 8B), resulting in a 60-fold reduction in the outlet's contributing area compared to a 3.5-fold reduction using the Borselli index. The marked reduction in contributing area at the outlet under the Revised Index method can be attributed to the combined effects of extensive fragmentation due to theoretical parcel divisions and land-use patterns in 2018.

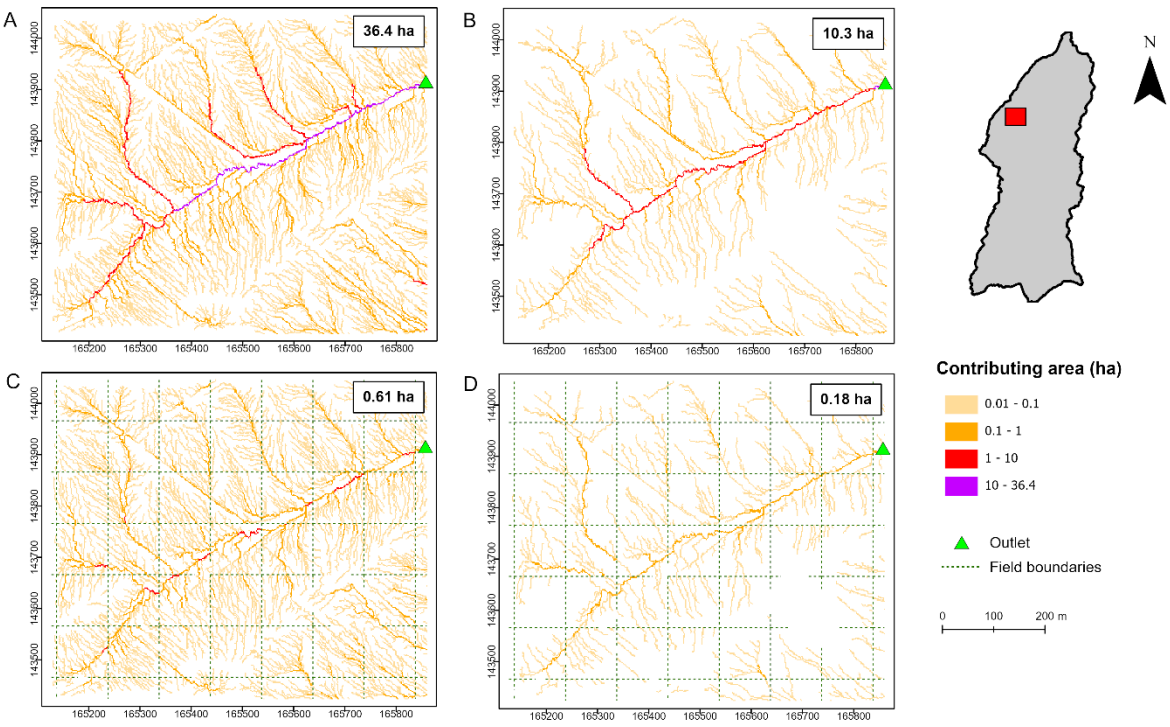

512 **Fig. 8.** Comparison of weighting methods for the contributing area included in the weighting factor (*W*) for
513 the upstream component of *IC* across a 45 ha area in the Dyle sub-catchment, based on 2018 land use and
514 calculated under four scenarios: A) unweighted, B) with the C factor weighting (Borselli index), C)
515 incorporating 30% connectivity at field boundaries for a hypothetical configuration fragmented into 1 ha
516 parcels, and D) combining both weightings (Revised index). The contributing area at the outlet is indicated
517 in the top right-hand corner. Longitude and latitude are in the Belgian Lambert 1972 projection system.
518
519
520 The comparison between the Borselli index (Fig. 9A) and the Revised index (Fig. 9B) for the same land use
521 highlights important patterns of sediment connectivity. For both indices, higher values are associated with
522 steep hillslope areas and along concentrated flow paths, particularly near the catchment outlet. These
523 findings align with previous studies that emphasise the role of topography in sediment dynamics (e.g.,
524 Calsamiglia et al., 2017, 2018). Notably, the mean and median IC values are higher for the Borselli index (-
525 7.04 and -6.69, respectively) compared to the Revised index (-7.36 and -7.18), reflecting the disconnection
526 effects induced by landscape fragmentation, specifically at field boundaries. As expected, fragmentation
527 reduces sediment connectivity along concentrated flow paths by interrupting sediment transfer and reducing

the effective slope length of runoff pathways. For example, studies such as Boardman and Vandaele (2010) and Golosov et al. (2024) have demonstrated how field boundaries and other linear structures can act as sediment traps, increasing deposition and mitigating sediment export. However, beyond these concentrated flow paths, the impact of fragmentation on connectivity appears more limited due to the uniformity of land uses across the catchment, which stabilises overall sediment dynamics. Consequently, the analysis will focus on two scales: along concentrated flow paths with a contributing area of at least 1 ha and over the whole catchment.

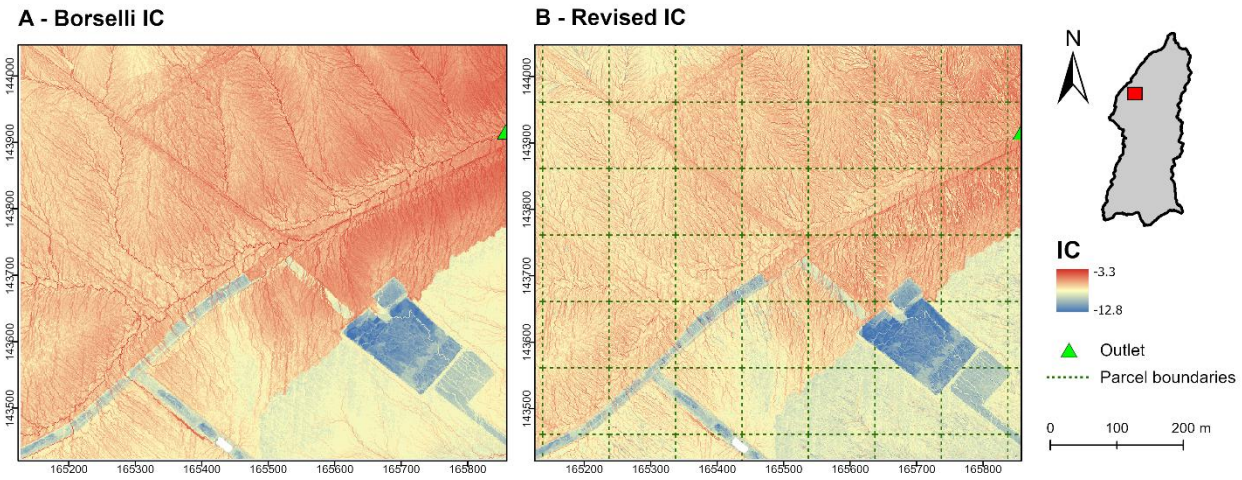

Fig. 9. Comparison of the Borselli connectivity index (A) and the Revised connectivity index applied to a hypothetical configuration fragmented into 1 ha parcels (B) for the 2018 land use in the Dyle sub-catchment. Coordinates are in the Belgian Lambert 1972 projection system.

The Revised connectivity index enables an in-depth analysis of the landscape patchiness by incorporating the effects of spatial land-use distribution and fragmentation.

Furthermore, this index revision can include additional vegetation barriers, such as hedgerows, expanding its application as demonstrated by studies like Gumiere et al. (2011) and Muñoz et al. (2024), which highlighted the impact of vegetation barriers on sediment trapping.

4.3. Validation results of connectivity

Data derived from aerial images and field observations were used to validate the results of IC in the Dyle sub-catchment (Fig. 10). Sediment deposits were identified upstream of linear landscape features (Fig. 10a), revealing several factors influencing deposition. Topography-controlled deposits were observed in flat areas,

along thalwegs, or at the bottom of slopes. Additionally, wooded strips acted as retention areas for sediment flows, as evidenced by multiple deposits located in these areas (Fig. 10c6). Deposition was also noted upstream of field boundaries (Fig. 10c3,4). These boundaries often featured downstream vegetation, such as crops, functioning as sediment barriers, as highlighted in studies by Beuselinck et al. (2000) and van Dijk et al. (2005). In such cases, connectivity was reduced. As highlighted by Beuselinck et al. (2000), deposition results from multiple factors. This is illustrated in photograph 1 (Fig. 10c), where the deposit is located within the thalweg upstream of a more developed maize crop, indicating that both topography and vegetation play a controlling role.

Conversely, gullies were observed along concentrated flow paths (Fig. 10c2,5). Landscape fragmentation appears to have an influence on gully control despite the intensity of the hydrological event. In line with studies by Beuselinck et al (2000) and Maugnard (2015), gullies end at field boundaries.

A comparison of the two indices in two deposition-prone zones underscores the differences in their connectivity patterns (Fig. 10b). In zone I, the Revised IC indicates a disconnection of sediment flows downstream of a field boundary along concentrated flow paths. This corresponds to the observed deposits upstream of the boundary, resulting from the vegetation barrier effect of the downstream crop. In zone II, deposits controlled by the wooded strip show reduced connectivity due to a combination of low C factor values and attenuation along concentrated flow paths. In contrast, the topography-controlled deposits in this zone were situated along a boundary between two fields with identical land use. Here, the reduced connectivity was primarily attributed to the flat terrain and a potential edge effect at the boundary, rather than the vegetation barrier effect assumed by the revised index at field boundaries.

In conclusion, the Revised IC produces generally more realistic connectivity maps in agricultural catchments. However, connectivity at field boundaries remains complex and challenging to evaluate, as not all boundaries act as effective sediment barriers. The analysis of functional connectivity following an extreme rainfall event suggests that parcel connectivity should be integrated into the revised index when field

boundaries are oriented perpendicular to flow paths and reinforced by dense vegetation cover downstream. Alternatively, field-based data should be utilized if available to ensure accuracy.

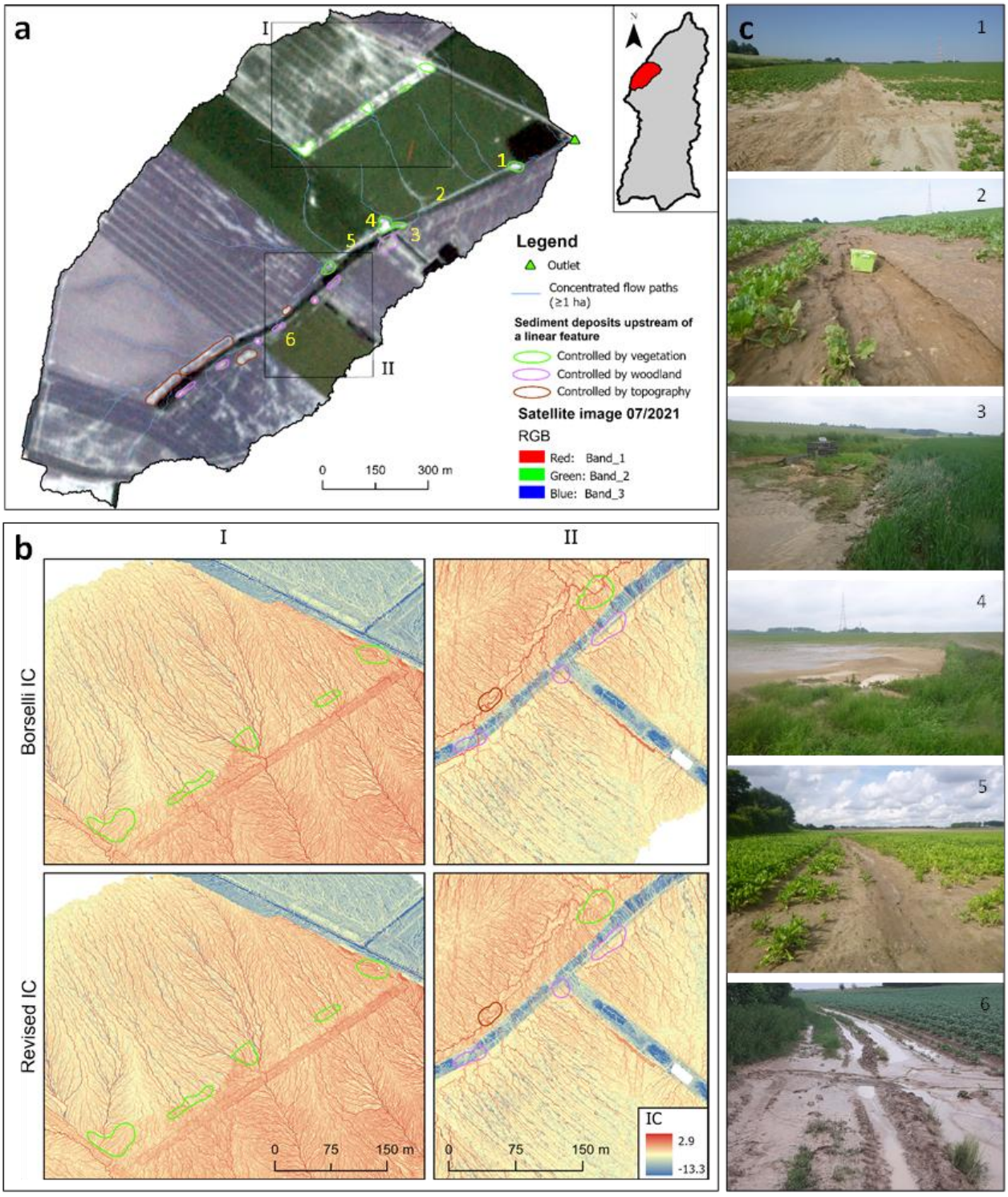

Fig. 10. (a) Satellite image from July 2021 displaying polygons that delineate sediment deposits located upstream of linear landscape features. (b) Changes in the spatial distribution of connectivity between

Borselli and Revised IC. (c) Photographs of deposits and gullies taken in July 2021.Comparative analysis of connectivity across diverse catchments.

The *IC* values range between -14.53 and 6.35 for the Scheldt sub-catchment, -14.89 and 6.79 for the Dyle sub-catchment, and between -15.17 and 6.79 for the Houyou sub-catchment (Table 6). The spatial distribution of *IC* is strongly influenced by slope gradient, general catchment morphology, the configuration of the natural drainage network, and surface characteristics such as surface roughness and land use (Calsamiglia et al., 2018). This explains why the Dyle sub-catchment (*KG* = 1.54) and Houyou sub-catchment (*KG* = 1.37), with their larger areas and elongated hydrographic networks, exhibit higher *IC* ranges compared to the smaller and more compact Scheldt sub-catchment (*KG* = 1.23). Additionally, the average gradients are steeper for the Houyou sub-catchment (6%), followed by the Dyle sub-catchment (5.5%), and finally the Scheldt sub-catchment (4.5%), further highlighting the differences between the Scheldt sub-catchment and the other two sub-catchments.

According to the main statistics (Table 6), *IC* values decrease as vegetation cover increases, reflecting a reduction in the C factor. As expected, in all three catchments, the ranking of land use scenarios from most connected to least connected is as follows: bare soil < spring crops < winter cereals < temporary grassland < permanent grassland. At the catchment scale, the *IC* distributions for the bare soil and permanent grassland scenarios represent the two extremes of connectivity, ranging from the most connected to the least connected scenarios in agricultural environments within these catchments (Table 6).

Table 6. Main statistics of *IC* across three sub-catchments for a range of land use (Borselli *IC*) and parcel arrangement scenarios for 2018 land use (Revised *IC*). The statistics encompass the range, the median (Q50), and standard deviation (stdev).

Scenarios	Scheldt			Dyle			Houyou		
	Range	Q50	Stdev	Range	Q50	Stdev	Range	Q50	Stdev
Land use – Borselli IC									
100% Bare soil	-14.36 – 6.35	-7.92	1.41 [a]	-14.89 – 6.79	-8.01	1.28 [a]	-14.96 – 6.79	-7.92	1.45 [a]
100% Spring row crops	-14.50 – 5.89	-8.40	1.41 [b]	-14.89 – 6.31	-8.60	1.26 [b]	-14.96 – 6.34	-8.41	1.45 [b]
100% Winter cereals	-14.50 – 5.69	-8.61	1.33 [c]	-14.89 – 6.11	-8.81	1.20 [c]	-14.96 – 6.14	-8.63	1.38 [c]

100% Temporary grassland	-14.50 – 5.29	-9.02	1.19 [d]	-14.89 – 5.71	-9.22	1.0 [d]	-14.98 – 5.75	-9.06	1.23 [d]
100% Permanent grassland	-14.53 – 4.34	-10.22	0.89 [e]	-14.89 – 4.78	-10.40	0.85 [e]	-15.17 – 4.81	-10.36	0.93 [e]
2018 land use	-14.53 – 5.20	-8.86	1.32 [f]	-14.89 – 6.16	-8.83	1.18 [f]	-15.04 – 6.06	-9.24	1.38 [f]
Parcel fragmentation – Revised IC									
2018 parcel configuration	-14.53 – 4.40	-8.86	1.31 [fg]	-14.89 – 4.82	-8.84	1.17 [g]	-15.04 – 4.54	-9.25	1.37 [fg]
5 m isolines	-14.53 – 4.82	-8.86	1.31 [fg]	-14.89 – 4.52	-8.84	1.16 [gh]	-15.04 – 4.69	-9.25	1.36 [g]
1 ha grid	-14.53 – 3.35	-8.87	1.30 [g]	-14.89 – 4.00	-8.84	1.15 [h]	-15.04 – 3.42	-9.25	1.35 [g]

[a,b,c,d,e,f,g,h] Two-sample Kolmogorov-Smirnov test for significant difference between two cumulative distributions.

Compared to the Borselli index (Fig. 11A), the Revised index is applied to three distinct fragmentation configurations while maintaining the same land use: the 2018 parcel configuration (Fig. 11B), a fragmentation layout based on boundaries aligned with 5 m isolines (Fig. 11C), and a regular 1 ha parcel grid (Fig. 11D). The primary statistics reveal that landscape fragmentation has only a minimal effect on median connectivity across the catchment, with *IC* variations of ≤0.01 between the unfragmented (Borselli *IC*) and most fragmented landscapes in all three catchments (Table 6). However, under the Revised index, maximum connectivity values, representing the most connected areas within the catchment, diminish as landscape fragmentation increases.

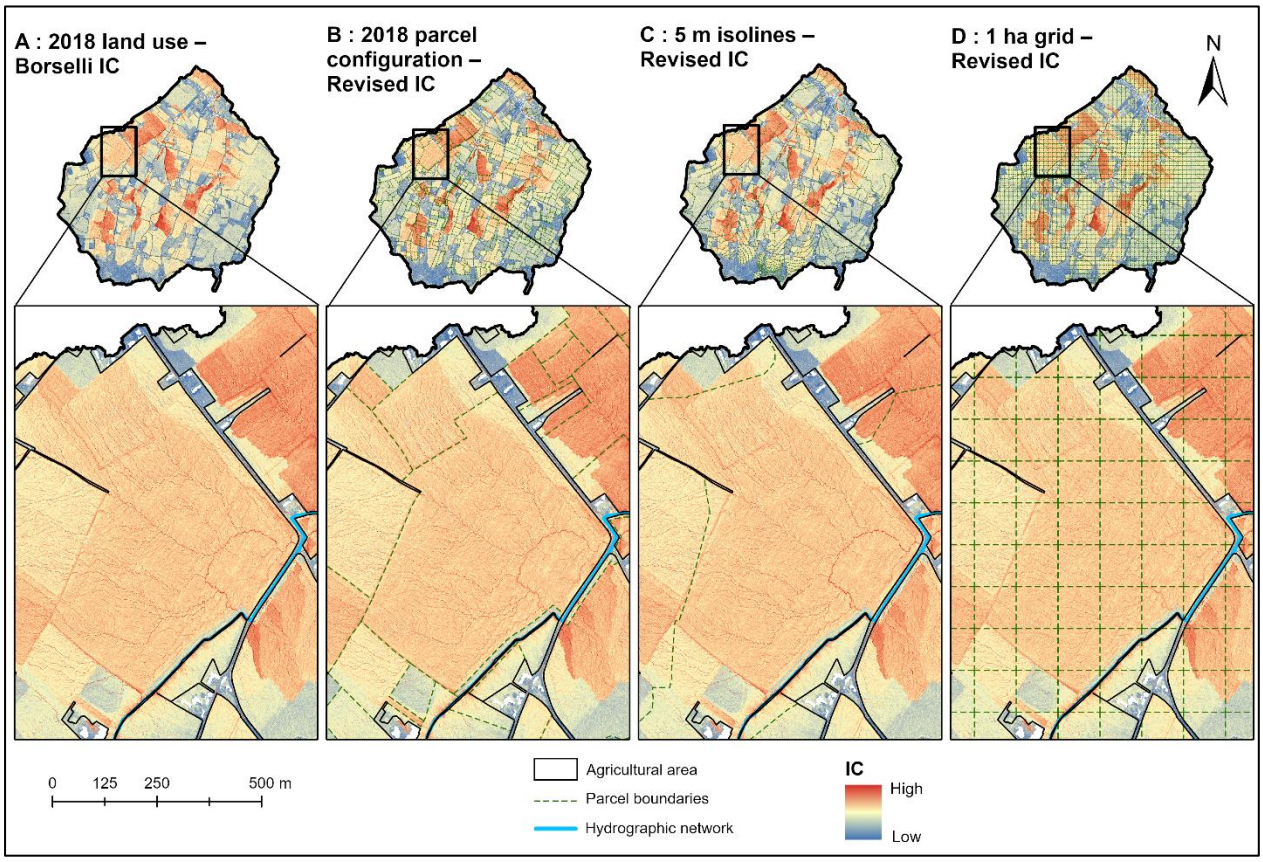

Fig.11. Spatial patterns of *IC* in the Scheldt sub-catchment with 2018 land use. The Borselli index (A) is compared with the Revised index applied to three different landscape fragmentation configurations: (B) fragmentation according to the 2018 parcel configuration, (C) fragmentation based on 5 m isolines, and (D) fragmentation into 1 ha parcels. The central parcel, depicted in figure B and occupying an area of 23 ha, is dedicated to the cultivation of potatoes.

In Figure 12, the analysis of the cumulative *IC* distribution provides an overview of the impacts of the different configurations on connectivity at the scale of the catchment and concentrated flow paths. A distribution that tends towards negative values indicates a preference for disconnection of flows across the landscape, while an inverse trend suggests an increase in connectivity.

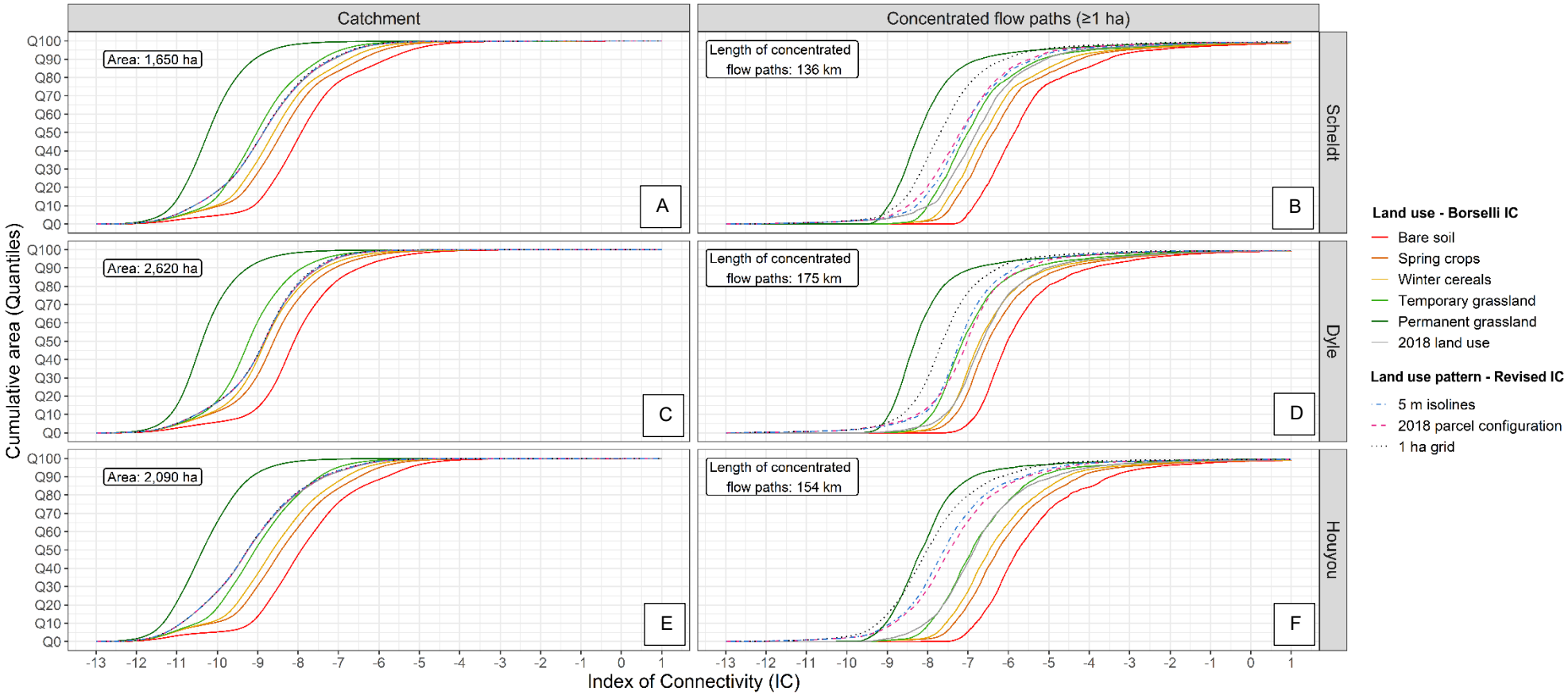

Fig.12. Cumulative distribution of *IC* values for different parcel and land use arrangement scenarios in the Scheldt, Dyle and Houyou sub-catchments. The scenarios examined include different land uses (Borselli index – bare soil, spring crops, winter cereals, temporary grassland, permanent grassland, and 2018 land use) and parcel arrangements for 2018 land use (Revised index – 2018 parcel configuration, 1 ha grid, and 5 m isolines). The land use for the different parcel arrangements corresponds to that of 2018. In each catchment, *IC* is presented at two distinct levels: at the overall scale of the catchment and at a finer level for concentrated flow paths with a contributing area of 1 ha or more. The area corresponding to the scale is framed in the top left-hand corner of each graph.

Impact of fragmentation at catchment scale

At the catchment scale (Fig. 12A, C, and E), the cumulative distribution of *IC* appears to be significantly shaped by land use, primarily because it affects a large surface area. The two-sample Kolmogorov–Smirnov (KS) test, which is sensitive to differences in both location and shape of the empirical cumulative distribution functions of the two samples, is employed to compare the IC cumulative distribution (Table 6). The KS test indicated significant differences between land use scenarios ($p < 0.05$). Consequently, land uses with more vegetation cover tend to better disconnect sediment flows within the landscape. Thus, the connectivity index distribution for the 2018 parcel configuration is heavily influenced by the land use of agricultural areas in 2018 across the three catchments. Significant differences in the 2018 land use among the three catchments result from a greater presence of forest in the Houyou sub-catchment, followed by the Dyle sub-catchment (Table 1); a higher percentage of spring crops, 11% and 9% more, respectively, in the Scheldt and the Dyle sub-catchments compared to the Houyou sub-catchment; and a lower percentage of grasslands in the Dyle sub-catchment. These differences account for the shifts observed in the connectivity distribution curve position for the 2018 land-use scenario across the three catchments (Fig. 12). We can quantify the disconnection between the 2018 land use and the temporary grassland scenario, whose C factor is on average at least two times lower in the three catchments (Table 3), by identifying the quantile at which the 2018 land use becomes less connected than temporary grassland. This corresponds to Q23 for the Scheldt sub-catchment, Q15 for the Dyle sub-catchment, and Q85 for the Houyou sub-catchment. In other words, the 2018 parcel configuration is 85% less connected than a configuration entirely covered by temporary grasslands in the Houyou sub-catchment. In terms of land use, the Dyle sub-catchment is the most at risk due to increased connectivity arising from lower soil vegetation cover, in contrast to the Houyou sub-catchment. These results show that the 2018 arrangement of agricultural land, with permanent grasslands strategically placed near waterways and on steep slopes, effectively disconnects landscape elements more than a scenario with uniform temporary grasslands, despite the latter covering a larger area on average. In line with our results, the studies by López-Vicente et al. (2013), Foerster et al. (2014), Gay et al. (2015), Najafi et al. (2021), and Wang and Zhang (2022) highlight that the spatial distribution and type of vegetation across the landscape is one of the most important factor in explaining changes in connectivity.

659

660 Visually, for the 2018 land-use data across the three catchments, the distributions of the Borselli *IC* and the
661 Revised *IC* are similar. The KS test results showed no significant difference ($p > 0.05$) in most cases between
662 the 2018 land use scenario (Borselli *IC*) and the fragmented parcel scenarios (Revised *IC*), suggesting only
663 minimal variation between the two indices. This finding is further supported by the close alignment of their
664 median values, as detailed in Table 6. This suggests that land use, which impacts all pixels across the
665 catchment, has a stronger overall influence on *IC* than landscape fragmentation. The latter, acting more
666 locally along field boundaries, primarily affects *IC* along concentrated flow paths (Fig. 12B, D, and F).

667

668 At the catchment scale, the cumulative distribution of the Borselli index in the Scheldt sub-catchment (i.e.,
669 without fragmentation) shows that the 5% least connected areas (Q5) have values below -11.04, while the
670 5% most connected areas (Q95) have values above -6.62 (Fig. 11A). For a higher threshold, the 10% least
671 connected areas (Q10) are below -10.57, and the 10% most connected areas (Q90) exceed -7.13. Using
672 these values as a reference to assess the impact of parcel fragmentation (Supplementary data – Fig. A1),
673 Q5 remain consistent across fragmented and non-fragmented configurations, while for Q10, the fragmented
674 configurations show slight increases in total surface area. Specifically, there is an increase of 0.016% for
675 the 1 ha parcel configuration, 0.007% for the 5 m isolines-based configuration, and 0.001% for the 2018
676 parcel configuration. For the most connected areas (Q90 and Q95), a reduction in surface area occurs
677 across all scenarios. For the 1 ha configuration, Q90 and Q95 decrease by 0.77% and 0.48%, respectively;
678 for the 5 m isolines-based configuration, they decrease by 0.35% and 0.20%; and for the 2018 parcel
679 configuration, by 0.29% and 0.20%.

680

681 The Dyle and Houyou sub-catchments follow a similar pattern, with disconnection effects being most
682 pronounced in the highly connected areas (Q90 and Q95). In these sub-catchments, the 1 ha parcel
683 configuration shows the highest disconnection, with Q90 decreasing by 1.13% and 0.80%, respectively.
684 Consistently, across all three catchments, the 1 ha parcel configuration exhibits the highest percentages of
685 disconnected areas for both the most and least connected areas. This can be attributed to the higher

686 fragmentation of this configuration, characterized by a greater density of field and parcel boundaries
687 (Table 7) and smaller average parcel sizes (Table 3).
688
689 **Table 7**. Parcel configurations characteristics in the sub-catchments [agricultural area (A), density of field
690 boundaries (L_b/A), number of parcels (n_p), and parcels density (n_p/A)].

Sub-catchment	5 m isolines		1 ha grid	
	L_b/A (m ha-1)	n_p/A (ha-1)	L_b/A (m ha-1)	n_p/A (ha-1)
Scheldt	53.3	0.19	192.6	0.81
Dyle	84.6	0.32	193.4	1.21
Houyou	96.3	0.28	201.0	1.21

691
692 The three catchments reveal that isoline-based fragmentation is generally more effective in disrupting
693 sediment flow connectivity than the 2018 parcel configuration. However, the configuration of parcels in 2018
694 is more fragmented in the Scheldt and Houyou sub-catchments and shows a comparable level of
695 fragmentation in the Dyle sub-catchment (Tables 5 and 7). This finding holds for both the least connected
696 areas (Q10) and the most connected areas (Q90 and Q95). Although this difference in disconnection is
697 minor, it underscores the superior orientation and positioning of boundaries in the isoline-based
698 fragmentation. Specifically, the field boundaries are perpendicular to the flow along their entire length,
699 optimizing their effectiveness. Additionally, when the terrain is steep, the slope length of parcels is reduced
700 due to the decreased spacing between isolines. This aligns with the findings of López-Vicente et al. (2021)
701 and Rosier et al. (2024), who demonstrated that priority locations for vegetated features are associated with
702 high upslope areas, thereby further enhancing the effectiveness of these configurations in runoff retention.
703
704 **Impact of fragmentation on concentrated flow paths**
705 The effects of patchiness, the spatial organisation of patches with different soil hydrological properties in the
706 landscape, influences connectivity by acting primarily at two levels: the spatial heterogeneity of crops,
707 characterized by distinct hydraulic properties, and landscape fragmentation resulting from the agricultural
708 parcel structure. Our study focuses primarily on the second aspect. The main statistics reveal that scenarios
709 incorporating parcel fragmentation yield lower maximum *IC* values than those based on land use alone

(Table 6). At the scale of concentrated flow paths, all three catchments exhibit a shift towards lower *IC* values as fragmentation intensifies (Fig. 12B, D and F). At this scale, the KS test indicated statistically significant differences in cumulative IC distributions across scenario pairs within each of the three sub-catchments. However, the Houyou sub-catchment was an exception: here, no significant difference was observed between the isoline-based fragmentation and the 2018 parcel configurations ($p = 0.105$). Fiener et al. (2011) also concluded that increased landscape patchiness and its associated structures significantly impact, primarily reducing, the potential for surface runoff generation in agricultural catchments, which is closely linked to sediment transfer.

Artifacts appear in urban areas due to the presence of buildings, which are excluded in the connectivity calculations. These artifacts introduce approximately 0.5% interference within the Scheldt sub-catchment, partly explaining why the 2018 land use scenario shows greater disconnection compared to the permanent grassland scenario (Fig. 12B). Sensitivity is heightened along concentrated flow paths, given that the number of pixels involved is far smaller (at least 100 times fewer) compared to the full catchment scale.

The effect of fragmentation is most pronounced on the least connected flow paths, peaking at a disconnection rate of 36.5% for Q30 in the Scheldt sub-catchment, 49.1% for Q20 in the Dyle sub-catchment, and 44.8% for Q20 in the Houyou sub-catchment (Fig. 13). In contrast, the effect is less pronounced on the most connected flow paths. This discrepancy arises because the key concentrated flow paths are not located within agricultural areas. Instead, these flow paths are typically found downstream of agricultural areas, in valleys, along roads, or at the interfaces between agricultural and non-agricultural land, making them less likely to intersect with field boundaries. Conversely, the less connected flow paths are often situated on arable land, where the influence of fragmentation is more marked. Additionally, the most connected flow paths mitigate the disconnection effects of fragmentation due to their large contributing areas, as a significant proportion of the contributing pixels are not subject to flow reduction caused by field boundaries.

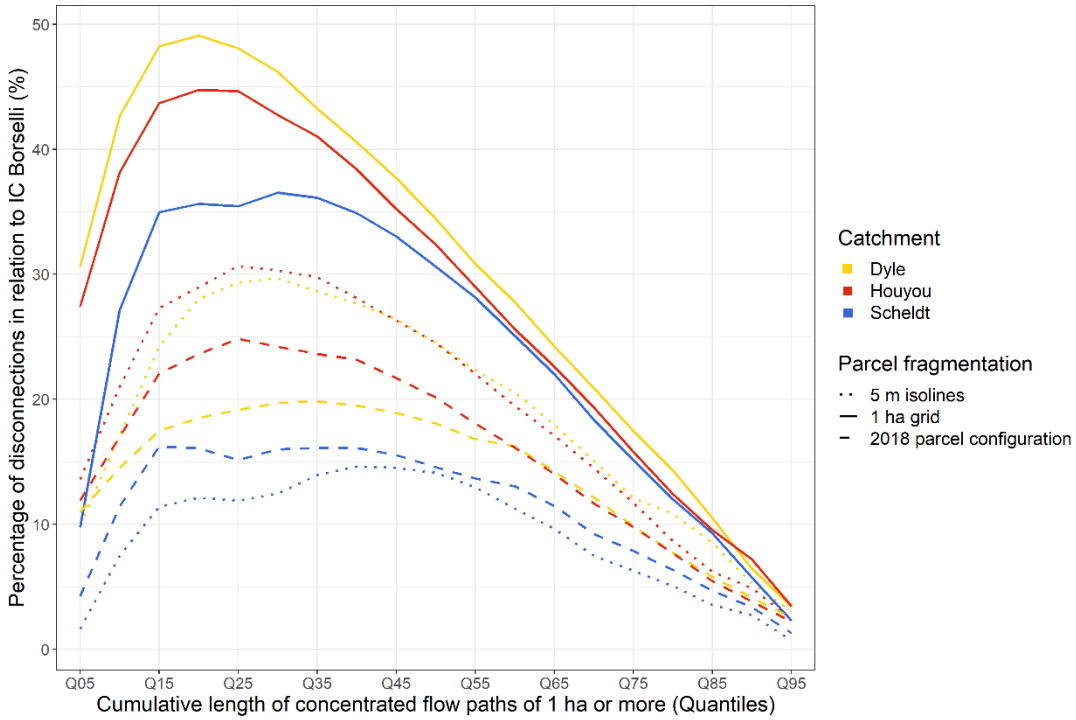

737 **Fig.13.** Percentage of disconnection in the length of concentrated flow paths induced by parcel
738 fragmentation (Revised *IC*) compared to an unfragmented landscape (Borselli *IC*) across the three studied
739 catchments, based on 2018 land use.

740

741 The most fragmented parcel configurations show better percentages of disconnection for both the most
742 connected and least connected areas (Fig. 13). The Dyle and Houyou sub-catchments show a better rate
743 of disconnection from fragmentation compared to the Scheldt. To compare disconnection efficiency, defined
744 as the ratio of the length of concentrated flow paths disconnected by fragmentation to the total length of field
745 boundaries (km km-1), we focus on the highest disconnection percentages (Q25) for the different
746 fragmentation scenarios. The disconnection efficiency ratios for the Scheldt, Dyle, and Houyou sub-
747 catchments are 0.171, 0.196, and 0.192 for the 1 ha grid fragmentation; 0.197, 0.216, and 0.248 for the
748 2018 parcel configuration; and 0.207, 0.273, and 0.275 for the isoline-based fragmentation, respectively.
749 This analysis reveals that the most fragmented configuration is not necessarily the most efficient. On
750 average, for the same length of field boundary, it disconnects a smaller proportion of concentrated flow
751 paths than other configurations. Notably, the isoline-based parcel fragmentation achieves the highest
752 disconnection efficiency across all three catchments. Additionally, when considering parcel size, the isoline-

based fragmentation proves advantageous: it features larger average parcel sizes compared to other scenarios, except in steep areas, while maintaining similar or superior disconnection efficiency ratios. This highlights that a landscape designed with larger parcels, strategically aligned with the topography, can achieve effective disconnection performance.

In addition to the sediment flow disconnection induced by fragmentation observed in our study, which is supported by the literature —such as Van Oost et al. (2000), who found that larger field sizes reduced field boundaries, increasing water erosion risk by 48%, and Li et al. (2020), who demonstrated that the enlargement of farm sizes significantly accelerates soil erosion— agronomic considerations must also be taken into account when organising an agricultural landscape. Increasing parcel size can maximise both production value and labour efficiency (*e.g.* Tilman et al., 2002), which explains why this strategy of expanding farm sizes has been widely adopted, particularly in Europe (Lowder et al., 2016). In this context, the isoline-based fragmentation offers the advantage of larger average parcel sizes, like or even larger than those in the 2018 configurations, with better disconnection performance at the catchment scale and along concentrated flow paths across all three catchments. Practical considerations of agricultural mechanization must also be addressed, particularly with contour farming.

In parallel with the analysis of potential vegetation barriers (Section 4.1), the Houyou sub-catchment exhibits the highest disconnection efficiency ratio for flow path length (0.248), which aligns with the highest density of potential vegetation barriers. Interestingly, despite the Scheldt sub-catchment having a seemingly more fragmented parcel configuration and a higher density of vegetation barriers compared to the Dyle sub-catchment, it shows the lowest disconnection efficiency ratio for the 2018 parcel configuration (0.197). The variation across different agricultural contexts and geomorphological settings, particularly the density of concentrated flow paths, adds complexity to cross-catchment comparisons, complicating the ability to draw generalized conclusions. When assessing the improvement in disconnection efficiency from the 2018 parcel configuration to the isoline-based fragmentation, the results reveal an efficiency increase of 5.5%, 26.3%, and 10.9% for the Scheldt, Dyle, and Houyou sub-catchments, respectively. This indicates that sub-catchments with more fragmented 2018 parcel configurations, such as the Scheldt sub-catchment,

experience smaller gains in disconnection efficiency when shifting to isoline-based fragmentation. Conversely, sub-catchments with less fragmented 2018 configurations, like the Dyle sub-catchment, show a more substantial increase in disconnection efficiency. This pattern suggests that initial landscape structure significantly influences the effectiveness of interventions aimed at enhancing hydrological disconnection.

The conclusions of this study are based on observations made in three catchments located in Belgium, characterised by relatively homogeneous lithological and climatic conditions, with silty soils and a temperate oceanic climate. IC is a measure of structural connectivity, independent of climatic and lithological factors, which are instead incorporated into functional connectivity. The methodology employed in this study is inherently structural and thus independent of climatic and lithological conditions, ensuring partial applicability to different contexts. The study must be coupled with functional connectivity to gain a better insight into actual sediment dynamics. Michalek et al. (2023) and Liu et al. (2024) emphasised that climatic factors — particularly changes in precipitation and temperature— will significantly affect sediment connectivity. Similarly, soil properties, such as texture, structure, and erodibility, play a pivotal role in sediment production and connectivity. For instance, erodible soils like silty loams prone to sealing amplify sediment transport, whereas soils with higher infiltration capacity reduce connectivity.

In the current methodology, the parcel connectivity factor is set at 30%, a value reflecting the regional climatic and lithological characteristics of the study areas. However, as demonstrated by Gumiere et al. (2011) and Muñoz et al. (2024), the efficiency of sediment trapping by plant barriers can vary considerably with climate. Muñoz et al. (2024) observed that plant barriers in semi-arid and arid climates have a higher sediment trapping efficiency (77.6%) compared to wet regions (55.1%), mainly due to differences in rainfall patterns. In humid regions, rainfall tends to be evenly distributed, increasing soil saturation, runoff, and sediment transport. Conversely, in semi-arid and arid climates, isolated storms and low soil saturation favour infiltration and reduce sediment detachment and transport. Adapting this parameter, P, to account for local conditions —such as rainfall intensity, soil properties, and vegetation dynamics— would enhance the robustness and applicability of the sediment connectivity framework to various regional contexts.

This study focused on theoretical parcel configurations that, while useful for understanding hypothetical land use scenarios, do not fully capture the complexities of real-world conditions. Future research should expand

this analysis to actual, existing parcel layouts to better grasp the practical implications and test the relationships between connectivity indices and erosion measurements in gauged catchments. Additionally, our modelling approach includes necessary simplifications, such as applying a uniform connectivity value of 30% across parcels regardless of vegetation cover on either side of field boundaries. These assumptions, while facilitating the modelling process, may overlook crucial nuances that impact sediment and water dynamics. This highlights the need for more sophisticated models that can account for the spatio-temporal variability of landscape connectivity. Future work should also investigate how optimising field boundaries can enhance flow disconnection across agricultural landscapes.

5. Conclusion

This study investigated the role of agricultural landscape features in shaping sediment connectivity across three agricultural catchments. Our findings indicate that the density of potential vegetation barriers in the landscape emerges as an indicator characterising agricultural landscape fragmentation. This density is influenced by the interaction between catchment morphology, the fragmentation of agricultural parcels, and the orientation of field boundaries relative to concentrated flow paths. Notably, more than one-third of these potential vegetation barriers consist of adjacent fields cultivated with the same crop type, including spring row crops, across all three catchments. This underscores the importance of implementing coordinated crop rotation strategies, particularly in critical areas along the flow paths.

In proposing a Revised connectivity index that incorporates both landscape fragmentation and vegetation cover, we underscore the significant impact of landscape fragmentation on sediment connectivity in agricultural catchments. Our findings demonstrate that this revised index enhances the mapping of connectivity by better capturing the influence of field boundaries and vegetation barriers. The Revised index demonstrates a trend towards lower *IC* values in fragmented configurations, indicating improved disconnection compared to the Borselli index. This disconnection is more evident along concentrated flow paths than at the catchment scale. At the catchment scale, although the differences in disconnection between various parcel fragmentation configurations are minor, the superior orientation and positioning of field boundaries in the isoline-based fragmentation are evident. For concentrated flow paths, the analysis

shows that the most fragmented configuration is not necessarily the most efficient. Across the three catchments, isoline-based fragmentation proves to be the most effective at disrupting sediment flow connectivity. On average, for an equivalent field boundary length, it disconnects a greater length of concentrated flow paths compared to other configurations. The isoline-based fragmentation offers a balance between larger average parcel sizes and effective disconnection, highlighting the importance of strategic landscape management in mitigating the trade-offs between agricultural productivity and environmental sustainability.

Acknowledgements

The research has been founded by the project Intell'eau, funded by the the Service Public de Wallonie.

References

Baartman, J.E.M., Masselink, R., Keesstra, S.D., Temme, A.J.A.M., 2013. Linking landscape morphological complexity and sediment connectivity. Earth Surf. Process. Landf. 38, 1457–1471. https://doi.org/10.1002/esp.3434

Baartman, J.E.M., Nunes, J.P., Masselink, R., Darboux, F., Bielders, C., Degré, A., Cantreul, V., Cerdan, O., Grangeon, T., Fiener, P., Wilken, F., Schindewolf, M., Wainwright, J., 2020. What do models tell us about water and sediment connectivity? Geomorphology 367, 107300. https://doi.org/10.1016/j.geomorph.2020.107300

Bakker, M.M., Govers, G., van Doorn, A., Quetier, F., Chouvardas, D., Rounsevell, M., 2008. The response of soil erosion and sediment export to land-use change in four areas of Europe: The importance of landscape pattern. Geomorphology, Human and climatic impacts on fluvial and hillslope morphology 98, 213–226. https://doi.org/10.1016/j.geomorph.2006.12.027

Batista, P.V.G., Fiener, P., Scheper, S., Alewell, C., 2022. A conceptual-model-based sediment connectivity assessment for patchy agricultural catchments. Hydrol. Earth Syst. Sci. 26, 3753–3770. https://doi.org/10.5194/hess-26-3753-2022

Beuselinck, L., Steegen, A., Govers, G., Nachtergaele, J., Takken, I., Poesen, J., 2000. Characteristics of sediment deposits formed by intense rainfall events in small catchments in the Belgian Loam Belt. Geomorphology 32, 69–82. https://doi.org/10.1016/S0169-555X(99)00068-9

Bielders, C.L., Ramelot, C., Persoons, E., 2003. Farmer perception of runoff and erosion and extent of flooding in the silt-loam belt of the Belgian Walloon Region. Environ. Sci. Policy, Socio-economic Factors in Soil Erosion and Conservation 6, 85–93. https://doi.org/10.1016/S1462-9011(02)00117-X

Boardman, J., 1988. Severe erosion on agricultural land in east Sussex, UK October 1987. Soil Technol. 1, 333–348. https://doi.org/10.1016/0933-3630(88)90013-X

Boardman, J., Vandaele, K., 2023. Soil erosion and runoff: The need to rethink mitigation strategies for sustainable agricultural landscapes in western Europe. Soil Use Manag. 39, 673–685. https://doi.org/10.1111/sum.12898

Boardman, J., Vandaele, K., 2016. Effect of the spatial organization of land use on muddy flooding from cultivated catchments and recommendations for the adoption of control measures. Earth Surf. Process. Landf. 41, 336–343. https://doi.org/10.1002/esp.3793

Boardman, J., Vandaele, K., 2010. Soil erosion, muddy floods and the need for institutional memory. Area 42, 502–513. https://doi.org/10.1111/j.1475-4762.2010.00948.x

Boardman, J., Vandaele, K., Evans, R., Foster, I.D.L., 2019. Off-site impacts of soil erosion and runoff: Why connectivity is more important than erosion rates. Soil Use Manag. 35, 245–256. https://doi.org/10.1111/sum.12496

Bormann, H., Breuer, L., Gräff, T., Huisman, J.A., 2007. Analysing the effects of soil properties changes associated with land use changes on the simulated water balance: A comparison of three hydrological catchment models for scenario analysis. Ecol. Model., Recent Developments in Hydrological Modelling towards Sustainable Catchment Management 209, 29–40. https://doi.org/10.1016/j.ecolmodel.2007.07.004

Borrelli, P., Alewell, C., Alvarez, P., Anache, J.A.A., Baartman, J., Ballabio, C., Bezak, N., Biddoccu, M., Cerdà, A., Chalise, D., Chen, S., Chen, W., De Girolamo, A.M., Gessesse, G.D., Deumlich, D., Diodato, N., Efthimiou, N., Erpul, G., Fiener, P., Freppaz, M., Gentile, F., Gericke, A., Haregeweyn, N., Hu, B., Jeanneau, A., Kaffas, K., Kiani-Harchegani, M., Villuendas, I.L., Li, C., Lombardo, L., López-Vicente, M., Lucas-Borja, M.E., Märker, M., Matthews, F., Miao, C., Mikoš, M., Modugno, S., Möller, M., Naipal, V., Nearing, M., Owusu, S., Panday, D., Patault, E., Patriche, C.V., Poggio, L., Portes, R., Quijano, L., Rahdari, M.R., Renima, M., Ricci, G.F., Rodrigo-Comino, J., Saia, S., Samani, A.N., Schillaci, C., Syrris, V., Kim, H.S., Spinola, D.N., Oliveira, P.T., Teng, H., Thapa, R., Vantas, K., Vieira, D., Yang, J.E., Yin, S., Zema, D.A., Zhao, G., Panagos, P., 2021. Soil erosion modelling: A global review and statistical analysis. Sci. Total Environ. 780, 146494. https://doi.org/10.1016/j.scitotenv.2021.146494

Borselli, L., Cassi, P., Torri, D., 2008. Prolegomena to sediment and flow connectivity in the landscape: A GIS and field numerical assessment. CATENA 75, 268–277. https://doi.org/10.1016/j.catena.2008.07.006

Bracken, L.J., Turnbull, L., Wainwright, J., Bogaart, P., 2015. Sediment connectivity: a framework for understanding sediment transfer at multiple scales. Earth Surf. Process. Landf. 40, 177–188. https://doi.org/10.1002/esp.3635

Brocca, L., Tullo, T., Melone, F., Moramarco, T., Morbidelli, R., 2012. Catchment scale soil moisture spatial–temporal variability. J. Hydrol. 422–423, 63–75. https://doi.org/10.1016/j.jhydrol.2011.12.039

Bronstert, A., Vollmer, S., Ihringer, J., 1995. A review of the impact of land consolidation on runoff production and flooding in Germany. Phys. Chem. Earth 20, 321–329. https://doi.org/10.1016/0079-1946(95)00044-5

Bucher, B., Demuth, S., 1985. Vergleichende Wasserbilanz eines flurbereinigten und eines nicht flurbereinigten Einzugsgebietes im Ostkaiserstuhl für den Zeitraum 1977–1980. Dtsch Gewässerkdl. Mitt 29, 1–4.

Calsamiglia, A., Fortesa, J., García-Comendador, J., Lucas-Borja, M.E., Calvo-Cases, A., Estrany, J., 2017. Spatial patterns of sediment connectivity in terraced lands: Anthropogenic controls of catchment sensitivity. Land Degrad. Dev. 29, 1198–1210. https://doi.org/10.1002/ldr.2840

Calsamiglia, A., García-Comendador, J., Fortesa, J., López-Tarazón, J.A., Crema, S., Cavalli, M., Calvo-Cases, A., Estrany, J., 2018. Effects of agricultural drainage systems on sediment connectivity in a small Mediterranean lowland catchment. Geomorphology 318, 162–171. https://doi.org/10.1016/j.geomorph.2018.06.011

Cantreul, V., Bielders, C., Calsamiglia, A., Degré, A., 2018. How pixel size affects a sediment connectivity index in central Belgium. Earth Surf. Process. Landf. 43, 884–893. https://doi.org/10.1002/esp.4295

Cantreul, V., Pineux, N., Swerts, G., Bielders, C., Degré, A., 2020. Performance of the LandSoil expert-based model to map erosion and sedimentation: application to a cultivated catchment in central Belgium. Earth Surf. Process. Landf. 45, 1376–1391. https://doi.org/10.1002/esp.4808

Cassi, P., 2010. Studio e parametrizzazione della connettività dei deflussi attraverso la definizione di un indice di connettività (Unpublished PhD). Facoltà di Agraria, Università degli Studi di Firenze, Italy. pp 123, Italy.

Cavalli, M., Crema, S., Marchi, L., 2014. Guidelines on the Sediment Connectivity ArcGis Toolbox and stand-alone application. https://doi.org/10.13140/RG.2.1.3243.5361

Cavalli, M., Trevisani, S., Comiti, F., Marchi, L., 2013. Geomorphometric assessment of spatial sediment connectivity in small Alpine catchments. Geomorphology, Sediment sources, source-to-sink fluxes and sedimentary budgets 188, 31–41. https://doi.org/10.1016/j.geomorph.2012.05.007

Cerdà, A., Flanagan, D.C., le Bissonnais, Y., Boardman, J., 2009. Soil erosion and agriculture. Soil Tillage Res. 106, 107–108. https://doi.org/10.1016/j.still.2009.10.006

Chartin, C., Evrard, O., Salvador-Blanes, S., Hinschberger, F., Van Oost, K., Lefèvre, I., Daroussin, J., Macaire, J.-J., 2013. Quantifying and modelling the impact of land consolidation and field borders on soil redistribution in agricultural landscapes (1954–2009). CATENA 110, 184–195. https://doi.org/10.1016/j.catena.2013.06.006

Devátý, J., Dostál, T., Hösl, R., Krása, J., Strauss, P., 2019. Effects of historical land use and land pattern changes on soil erosion – Case studies from Lower Austria and Central Bohemia. Land Use Policy 82, 674–685. https://doi.org/10.1016/j.landusepol.2018.11.058

Dotterweich, M., 2008. The history of soil erosion and fluvial deposits in small catchments of central Europe: Deciphering the long-term interaction between humans and the environment — A review. Geomorphology, The 39th Annual Binghamton Geomorphology Symposium: Fluvial Deposits and Environmental History: Geoarchaeology, Paleohydrology, and Adjustment to Environmental Change 101, 192–208. https://doi.org/10.1016/j.geomorph.2008.05.023

Evans, R., 2006. Curtailing water erosion of cultivated land: an example from north Norfolk, eastern England. Earth Surf. Process. Landf. 31, 598–605. https://doi.org/10.1002/esp.1354

Evrard, O., Bielders, C.L., Vandaele, K., van Wesemael, B., 2007. Spatial and temporal variation of muddy floods in central Belgium, off-site impacts and potential control measures. CATENA 70, 443–454. https://doi.org/10.1016/j.catena.2006.11.011

Evrard, O., Vandaele, K., Bielders, C., Wesemael, B. van, 2008. Seasonal evolution of runoff generation on agricultural land in the Belgian loess belt and implications for muddy flood triggering. Earth Surf. Process. Landf. 33, 1285–1301. https://doi.org/10.1002/esp.1613

Farahani, S.S., Fard, F.S., Asoodar, M.A., 2016. Effects of contour farming on runoff and soil erosion reduction: a review study. Elixir Agric. 101, 44089–44093.

Fiener, P., Auerswald, K., Van Oost, K., 2011. Spatio-temporal patterns in land use and management affecting surface runoff response of agricultural catchments—A review. Earth-Sci. Rev. 106, 92–104. https://doi.org/10.1016/j.earscirev.2011.01.004

Fiener, P., Wilken, F., Auerswald, K., 2019. Filling the gap between plot and landscape scale – eight years of soil erosion monitoring in 14 adjacent watersheds under soil conservation at Scheyern, Southern Germany, in: Advances in Geosciences. Presented at the Innovative monitoring techniques and modelling approaches for analysing hydrological processes in small basins - 17th Biennial Conference ERB 2018, Darmstadt, Germany, 11–14 September 2018, Copernicus GmbH, pp. 31–48. https://doi.org/10.5194/adgeo-48-31-2019

Foerster, S., Wilczok, C., Brosinsky, A., Segl, K., 2014. Assessment of sediment connectivity from vegetation cover and topography using remotely sensed data in a dryland catchment in the Spanish Pyrenees. J. Soils Sediments 14, 1982–2000. https://doi.org/10.1007/s11368-014-0992-3

Fohrer, N., Haverkamp, S., Frede, H.-G., 2005. Assessment of the effects of land use patterns on hydrologic landscape functions: development of sustainable land use concepts for low mountain range areas. Hydrol. Process. 19, 659–672. https://doi.org/10.1002/hyp.5623

Follain, S., Minasny, B., McBratney, A.B., Walter, C., 2006. Simulation of soil thickness evolution in a complex agricultural landscape at fine spatial and temporal scales. Geoderma, Advances in landscape-scale soil research 133, 71–86. https://doi.org/10.1016/j.geoderma.2006.03.038

Golosov, V.N., Shamshurina, E.N., Kolos, G.I., Petel'ko, A.I., Zhidkin, A.P., 2024. Spatiotemporal Changes in the Erosion and Deposition Processes in a Small Catchment in the North of the Central Russian Upland. Eurasian Soil Sci. 57, 838–852. https://doi.org/10.1134/S1064229323603682

Gumiere, S.J., Le Bissonnais, Y., Raclot, D., Cheviron, B., 2011. Vegetated filter effects on sedimentological connectivity of agricultural catchments in erosion modelling: a review. Earth Surf. Process. Landf. 36, 3–19. https://doi.org/10.1002/esp.2042

Heckmann, T., Cavalli, M., Cerdan, O., Foerster, S., Javaux, M., Lode, E., Smetanová, A., Vericat, D., Brardinoni, F., 2018. Indices of sediment connectivity: opportunities, challenges and limitations. Earth-Sci. Rev. 187, 77–108. https://doi.org/10.1016/j.earscirev.2018.08.004

Hooke, J., Souza, J., 2021. Challenges of mapping, modelling and quantifying sediment connectivity. Earth-Sci. Rev. 223, 103847. https://doi.org/10.1016/j.earscirev.2021.103847

Jenson, S.K., Domingue, J.O., 1988. Extracting topographic structure from digital elevation data for geographic information system analysis. Photogramm. Eng. Remote Sens. 54, 1593–1600.

Keesstra, S., Nunes, J.P., Saco, P., Parsons, T., Poeppl, R., Masselink, R., Cerdà, A., 2018. The way forward: Can connectivity be useful to design better measuring and modelling schemes for water and sediment dynamics? Sci. Total Environ. 644, 1557–1572. https://doi.org/10.1016/j.scitotenv.2018.06.342

Keesstra, S.D., van Dam, O., Verstraeten, G., van Huissteden, J., 2009. Changing sediment dynamics due to natural reforestation in the Dragonja catchment, SW Slovenia. CATENA 78, 60–71. https://doi.org/10.1016/j.catena.2009.02.021

Lal, R., 1998. Soil erosion impact on agronomic productivity and environment quality. Crit. Rev. Plant Sci. 17, 319–464. https://doi.org/10.1080/07352689891304249

Lambert, A.M., 1963. Farm Consolidation in Western Europe. Geography 48, 31–48.

Li, Y., Tang, C., Huang, Z., Hussain, Z., Are, K.S., Abegunrin, T.P., Qin, Z., Guo, H., 2020. Increase in farm size significantly accelerated stream channel erosion and associated nutrient losses from an intensive agricultural watershed. Agric. Ecosyst. Environ. 295, 106900. https://doi.org/10.1016/j.agee.2020.106900

Lidberg, W., Ågren, A., Nilsson, M., Lundmark, T., 2017. Evaluating pre-processing methods of digital elevation models for hydrological modelling. Hydrol. Process. 31. https://doi.org/10.1002/hyp.11385

Liu, C., Chen, Y., Fang, G., Li, Z., Liu, Y., 2024. Impact of climatic and geomorphologic drivers on sediment connectivity in the Tarim River Basin, China. J. Hydrol. 643, 132027. https://doi.org/10.1016/j.jhydrol.2024.132027

López-Vicente, M., Kramer, H., Keesstra, S., 2021. Effectiveness of soil erosion barriers to reduce sediment connectivity at small basin scale in a fire-affected forest. J. Environ. Manage. 278, 111510. https://doi.org/10.1016/j.jenvman.2020.111510

López-Vicente, M., Poesen, J., Navas, A., Gaspar, L., 2013. Predicting runoff and sediment connectivity and soil erosion by water for different land use scenarios in the Spanish Pre-Pyrenees. CATENA, Scales in Soil Erosion 102, 62–73. https://doi.org/10.1016/j.catena.2011.01.001

Lowder, S.K., Skoet, J., Raney, T., 2016. The Number, Size, and Distribution of Farms, Smallholder Farms, and Family Farms Worldwide. World Dev. 87, 16–29. https://doi.org/10.1016/j.worlddev.2015.10.041
Luft, G., Morgenschweis, G., Keller, R., 1981. Auswirkungen von Grossterrassierungen auf hydrologische Prozesse in Istkaiserstuhl. Wasser Boden.
Maugnard, A., 2015. Characterization and prediction of ephemeral gully erosion in Wallonia (PhD). Université Catholique de Louvain, Louvain-la-Neuve.
Maugnard, A., Bielders, C., Bock, L., Colinet, G., Cordonnier, H., Degre, A., Demarcin, P., Dewez, A., Feltz, N., Legrain, X., Pineux, N., Mokadem, A., 2013. Cartographie du risque d'érosion hydrique à l'échelle parcellaire en soutien à la politique agricole wallonne (Belgique). Etude Gest. Sols 20, 127–141.
Maugnard, A., Cordonnier, H., Degre, A., Demarcin, P., Pineux, N., Bielders, C.L., 2014. Uncertainty assessment of ephemeral gully identification, characteristics and topographic threshold when using aerial photographs in agricultural settings. Earth Surf. Process. Landf. 39, 1319–1330. https://doi.org/10.1002/esp.3526
Mekonnen, M., Keesstra, S.D., Stroosnijder, L., Baartman, J.E.M., Maroulis, J., 2015. Soil Conservation Through Sediment Trapping: A Review. Land Degrad. Dev. 26, 544–556. https://doi.org/10.1002/ldr.2308
Michalek, A.T., Villarini, G., Husic, A., 2023. Climate change projected to impact structural hillslope connectivity at the global scale. Nat. Commun. 14, 6788. https://doi.org/10.1038/s41467-023-42384-2
Muñoz, J.-A., Guzmán, G., Soriano, M.-A., Gómez, J.A., 2024. Appraising trapping efficiency of vegetative barriers in agricultural landscapes: Strategy based on a probabilistic approach based on a review of available information. Int. Soil Water Conserv. Res. 12, 615–634. https://doi.org/10.1016/j.iswcr.2023.12.001
Najafi, S., Dragovich, D., Heckmann, T., Sadeghi, S.H., 2021. Sediment connectivity concepts and approaches. CATENA 196, 104880. https://doi.org/10.1016/j.catena.2020.104880
Nearing, M.A., Pruski, F.F., O'Neal, M.R., 2004. Expected climate change impacts on soil erosion rates: A review. J. Soil Water Conserv. 59, 43–50.
O'Callaghan, J.F., Mark, D.M., 1984. The extraction of drainage networks from digital elevation data. Comput. Vis. Graph. Image Process. 28, 323–344. https://doi.org/10.1016/S0734-189X(84)80011-0
Oorts, K., Buyle, S., Deproost, P., Swerts, M., 2020. Eindrapport potentiële bodemerosiekaart per perceel (2018). Departement Omgeving, Brussel.
Panagos, P., Ballabio, C., Meusburger, K., Spinoni, J., Alewell, C., Borrelli, P., 2017. Towards estimates of future rainfall erosivity in Europe based on REDES and WorldClim datasets. J. Hydrol. 548, 251–262. https://doi.org/10.1016/j.jhydrol.2017.03.006
Panagos, P., Borrelli, P., Poesen, J., Ballabio, C., Lugato, E., Meusburger, K., Montanarella, L., Alewell, C., 2015. The new assessment of soil loss by water erosion in Europe. Environ. Sci. Policy 54, 438–447. https://doi.org/10.1016/j.envsci.2015.08.012
Powlson, D.S., Gregory, P.J., Whalley, W.R., Quinton, J.N., Hopkins, D.W., Whitmore, A.P., Hirsch, P.R., Goulding, K.W.T., 2011. Soil management in relation to sustainable agriculture and ecosystem services. Food Policy, The challenge of global food sustainability 36, S72–S87. https://doi.org/10.1016/j.foodpol.2010.11.025
Prasuhn, V., Liniger, H., Gisler, S., Herweg, K., Candinas, A., Clément, J.-P., 2013. A high-resolution soil erosion risk map of Switzerland as strategic policy support system. Land Use Policy 32, 281–291. https://doi.org/10.1016/j.landusepol.2012.11.006
Radoux, J., Bourdouxhe, A., Coppée, T., De Vroey, M., Dufrêne, M., Defourny, P., 2022. A Consistent Land Cover Map Time Series at 2 m Spatial Resolution—The LifeWatch 2006-2015-2018-2019 Dataset for Wallonia. Data 8, 13. https://doi.org/10.3390/data8010013
Renard, K.G., 1997. Predicting Soil Erosion by Water: A Guide to Conservation Planning with the Revised Universal Soil Loss Equation (RUSLE). U.S. Department of Agriculture, Agricultural Research Service.
Rosier, I., Diels, J., Somers, B., Van Orshoven, J., 2024. Maximising runoff retention by vegetated landscape elements positioned through spatial optimisation. Landsc. Urban Plan. 243, 104968. https://doi.org/10.1016/j.landurbplan.2023.104968

Ryken, N., Vanden Nest, T., Al-Barri, B., Blake, W., Taylor, A., Bodé, S., Ruysschaert, G., Boeckx, P., Verdoodt, A., 2018. Soil erosion rates under different tillage practices in central Belgium : new perspectives from a combined approach of rainfall simulations and ^{7}Be measurements. SOIL TILLAGE Res. 179, 29–37. https://doi.org/10.1016/j.still.2018.01.010

Sharpley, A.N., Chapra, S.C., Wedepohl, R., Sims, J.T., Daniel, T.C., Reddy, K.R., 1994. Managing Agricultural Phosphorus for Protection of Surface Waters: Issues and Options. J. Environ. Qual. 23, 437–451. https://doi.org/10.2134/jeq1994.00472425002300030006x

Soille, P., 2004. Optimal removal of spurious pits in grid digital elevation models. Water Resour. Res. 40. https://doi.org/10.1029/2004WR003060

Strauss, V., Paul, C., Dönmez, C., Löbmann, M., Helming, K., 2023. Sustainable soil management measures: a synthesis of stakeholder recommendations. Agron. Sustain. Dev. 43, 17. https://doi.org/10.1007/s13593-022-00864-7

Swerts, M., Broekaert, S., Deproost, P., Renders, D., Oorts, K., 2020. Bodemerosierisico-indicator Vlaanderen 2008-2019. Departement Omgeving, Brussel.

Szilassi, P., Jordan, G., van Rompaey, A., Csillag, G., 2006. Impacts of historical land use changes on erosion and agricultural soil properties in the Kali Basin at Lake Balaton, Hungary. CATENA, Soil Erosion Research in Europe 68, 96–108. https://doi.org/10.1016/j.catena.2006.03.010

Takken, I., Beuselinck, L., Nachtergaele, J., Govers, G., Poesen, J., Degraer, G., 1999. Spatial evaluation of a physically-based distributed erosion model (LISEM). CATENA 37, 431–447. https://doi.org/10.1016/S0341-8162(99)00031-4

Tilman, D., Cassman, K.G., Matson, P.A., Naylor, R., Polasky, S., 2002. Agricultural sustainability and intensive production practices. Nature 418, 671–677. https://doi.org/10.1038/nature01014

Ulén, B., Bechmann, M., Oygarden, L., Kyllmar, K., 2012. Soil erosion in Nordic countries – future challenges and research needs. Acta Agric. Scand. 62. https://doi.org/10.1080/09064710.2012.712862

van Dijk, P.M., Auzet, A.-V., Lemmel, M., 2005. Rapid assessment of field erosion and sediment transport pathways in cultivated catchments after heavy rainfall events. Earth Surf. Process. Landf. 30, 169–182. https://doi.org/10.1002/esp.1182

Van Oost, K., Govers, G., Desmet, P., 2000. Evaluating the effects of changes in landscape structure on soil erosion by water and tillage. Landsc. Ecol. 15, 577–589. https://doi.org/10.1023/A:1008198215674

Verheijen, F.G.A., Jones, R.J.A., Rickson, R.J., Smith, C.J., 2009. Tolerable versus actual soil erosion rates in Europe. Earth-Sci. Rev. 94, 23–38. https://doi.org/10.1016/j.earscirev.2009.02.003

Verstraeten, G., Poesen, J., 1999. The nature of small-scale flooding, muddy floods and retention pond sedimentation in central Belgium. Geomorphology 29, 275–292. https://doi.org/10.1016/S0169-555X(99)00020-3

Verstraeten, G., Poesen, J., Goossens, D., Gillijns, K., Bielders, C., Gabriels, D., Ruysschaert, G., Van Den Eeckhaut, M., Vanwalleghem, T., Govers, G., 2006. Belgium, in: Soil Erosion in Europe. John Wiley & Sons, Ltd, pp. 385–411. https://doi.org/10.1002/0470859202.ch30

Vigiak, O., Borselli, L., Newham, L.T.H., McInnes, J., Roberts, A.M., 2012. Comparison of conceptual landscape metrics to define hillslope-scale sediment delivery ratio. Geomorphology 138, 74–88. https://doi.org/10.1016/j.geomorph.2011.08.026

Wang, C., Zhang, G., 2022. Spatial variation in sediment connectivity of small watershed along a regional transect on the Loess Plateau. CATENA 217, 106473. https://doi.org/10.1016/j.catena.2022.106473

Wischmeier, W.H., Smith, D.D., 1978. Predicting Rainfall Erosion Losses: A Guide to Conservation Planning. Department of Agriculture, Science and Education Administration.

Wohl, E., Brierley, G., Cadol, D., Coulthard, T.J., Covino, T., Fryirs, K.A., Grant, G., Hilton, R.G., Lane, S.N., Magilligan, F.J., Meitzen, K.M., Passalacqua, P., Poeppl, R.E., Rathburn, S.L., Sklar, L.S., 2019. Connectivity as an emergent property of geomorphic systems. Earth Surf. Process. Landf. 44, 4–26. https://doi.org/10.1002/esp.4434

Zanandrea, F., Michel, G.P., Kobiyama, M., 2020. Impedance influence on the index of sediment connectivity in a forested mountainous catchment. Geomorphology 351, 106962. https://doi.org/10.1016/j.geomorph.2019.106962

Zema, D. a., Bingner, R. l., Denisi, P., Govers, G., Licciardello, F., Zimbone, S. m., 2012. Evaluation of runoff, peak flow and sediment yield for events simulated by the AnnAGNPS model in a belgian agricultural watershed. Land Degrad. Dev. 23, 205–215. https://doi.org/10.1002/ldr.1068

Zhao, D., Jiao, Y., He, K., Xiong, D., Zhang, B., 2024. Evaluating the effect of natural-artificial linear landscape elements on flow and sediment connectivity in a typical agricultural terraced catchment, China. CATENA 234, 107561. https://doi.org/10.1016/j.catena.2023.107561

Ziegler, A.D., Giambelluca, T.W., Plondke, D., Leisz, S., Tran, L.T., Fox, J., Nullet, M.A., Vogler, J.B., Minh Troung, D., Tran Duc Vien, 2007. Hydrological consequences of landscape fragmentation in mountainous northern Vietnam: Buffering of Hortonian overland flow. J. Hydrol. 337, 52–67. https://doi.org/10.1016/j.jhydrol.2007.01.031

Supplementary data

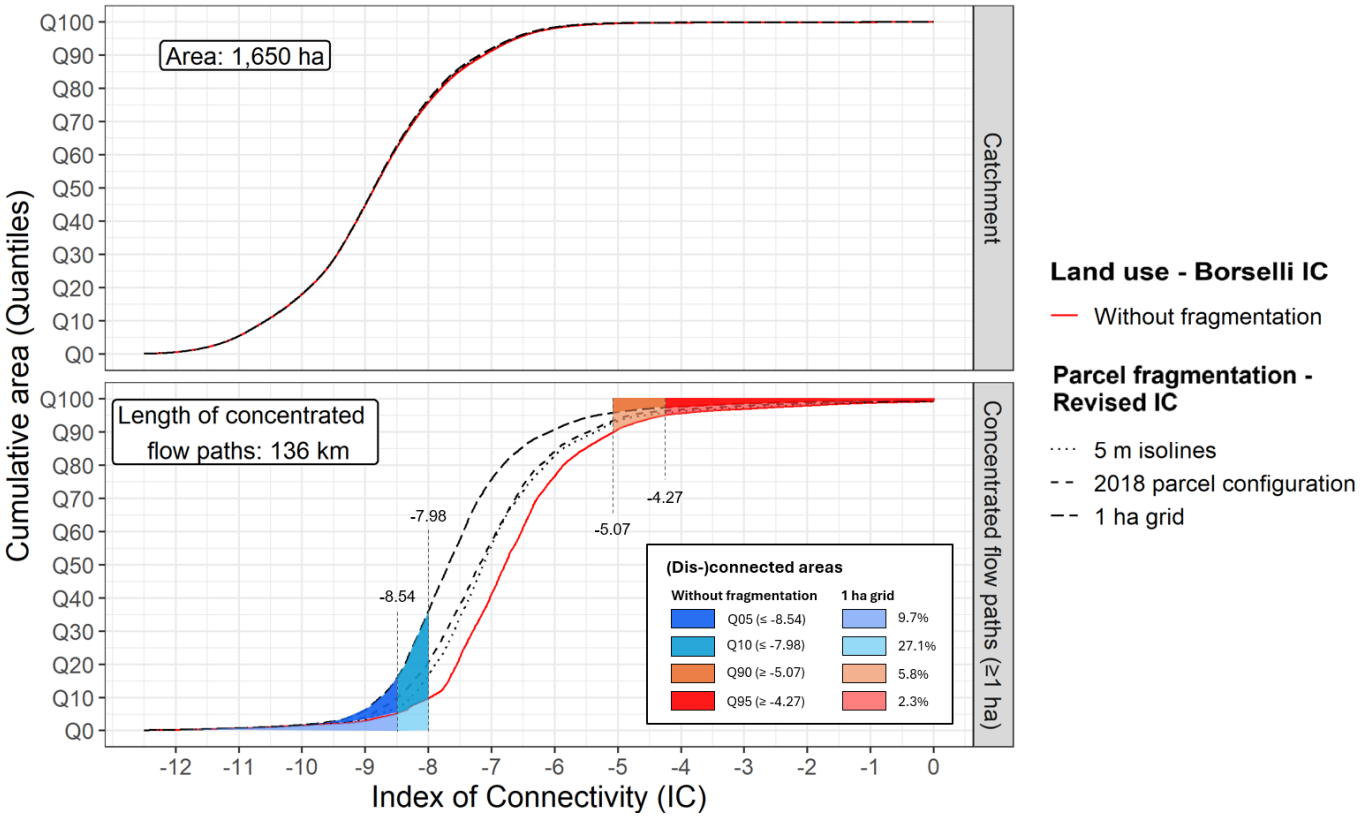

Fig. A1. Cumulative distribution of *IC* values in the Scheldt sub-catchment on 2018 land use for three parcel configurations: the Revised index for 1 ha parcels, the Revised index for the 2018 parcel configuration, and the Revised index for fragmented parcels based on 5 m isolines, alongside the Borselli index without fragmentation. The thresholds established, corresponding to 5% and 10% of the zones with lower (i.e. Q5 and Q10) and higher (Q90 and Q95) values for the Borselli index, make it possible to observe the differences between the most disconnected zones (in blue colours) and the most connected zones (in red colours) between two configurations. *IC* values are presented at two scales: the overall catchment scale and a finer scale for concentrated flow paths with an upstream area of 1 hectare or more. The area covered by each scale is highlighted in the top left-hand corner of each graph.